



# Numerical investigation of a smart window system with thermotropic Parallel Slat Transparent Insulation Material for building energy conservation and daylight autonomy

Yanyi Sun<sup>\*</sup>, Robin Wilson, Hao Liu, Yupeng Wu<sup>\*\*</sup>

Department of Architecture and Built Environment, Faculty of Engineering, University of Nottingham, Nottingham, UK

## ARTICLE INFO

### Keywords:

Thermotropic material  
Parallel slat transparent insulation materials (PS-TIM)  
Building energy conservation  
Automatic daylight regulation  
Building simulation

## ABSTRACT

Smart window designs have emerged as a means of providing dynamic regulation of solar energy and daylight, enhancing indoor comfort, and achieving building energy conservation. We evaluated a novel window design that integrated a thermotropic (TT) material and Transparent Insulation Material (TIM) and present the investigation in this paper. The Parallel Slat TIM (PS-TIM) structure contained within the window unit provides extra thermal resistance and helps to redirect daylight. The TT material, which is applied to the slats, provides automatic daylight and solar adjustment. Firstly, the TT PS-TIM window system has been characterised thermally and optically. Then, a comprehensive approach including both building energy and daylight simulation packages was used to predict building performance. The effects of geometry (i.e. slat spacing and slat tilt angle) and thermotropic features (i.e. transition temperature and optical properties) on building performance were investigated. The simulation results show that use of TT PS-TIM window system with carefully selected features can simultaneously improve building energy efficiency (up to 22% saving when compared with a conventional double-glazed (DG) window) and attain homogenous daylight distribution with an average Useful Daylight Illuminance, UDI<sub>500-2000 lux</sub>, of 52.2%. It was also found that both the geometric configurations and thermotropic features of a TT PS-TIM have significant influence on energy and daylight performance. TT PS-TIM with horizontally placed slats performs better than the unit with tilted slats, in terms of balance between energy efficiency and daylight availability. This research provides design guidance and material development suggestions for integration of this novel window system in buildings.

## 1. Introduction

Windows play an important role in determining the energy consumption and indoor environmental quality of the building they serve [1–3]. A properly designed window offers the potential to admit sufficient solar energy and daylight for passive heating and natural lighting, minimize undesirable heat losses to offer savings in heating energy, avoid overheating and glare, and facilitate satisfactory views into and out of a building [3–6].

Smart switchable windows, such as Electrochromic (EC) glazing, Thermochromic (TC) glazing and Thermotropic (TT) glazing, provide the potential to dynamically regulate solar and daylight transmittance in response to a varying external environment [7–11]. These can allow passive solar gains and/or daylight to be transmitted effectively when

desired, and attenuate them to prevent overheating and/or glare when not desired. TT materials are a form of chromogenic substance that can reversibly change its light transmission behaviour in response to a varying environment [8,12,13]. The transition from a highly transparent state to a strongly scattering, translucent state requires neither a power supply nor an active control unit, and depends solely on the temperature of the thermotropic layer [14,15]. When the temperature is lower than the design threshold switching temperature, the two main components of a thermotropic layer (i.e. polymer and water) are homogeneously mixed and their refractive indices ( $n$ ) are closely matched, resulting in a clear appearance with a transmittance of over 85% [13]. This state, when used in building window applications, allows transmittance of solar radiation and natural daylight, contributing to passive solar heat gain and savings in artificial-lighting energy. At temperatures above the design threshold switching temperature, the

\* Corresponding author.

\*\* Corresponding author.

E-mail addresses: [Yanyi.Sun@nottingham.ac.uk](mailto:Yanyi.Sun@nottingham.ac.uk) (Y. Sun), [Yupeng.Wu@nottingham.ac.uk](mailto:Yupeng.Wu@nottingham.ac.uk) (Y. Wu).

## Nomenclature

### Abbreviations

ASHRAE	American Society of Heating, Refrigerating and Air-Conditioning Engineers
BSDF	Bidirectional Scattering Distribution Function
CIBSE	Chartered Institution of Building Services Engineers
CFD	Computational Fluid Dynamics
DG	Double-glazed
EC	Electrochromic
EMS	Energy Management System
HPC	Hydroxypropyl cellulose
HVAC	Heating, ventilation, and air conditioning
IWEC	International Weather for Energy Calculation
PS-TIM	Parallel Slat Transparent Insulation Materials
PMMA	Polymethylmethacrylate
pNIPAm	Poly(N-isopropylacrylamide)
pNIPAm-AEMA	Poly(N-isopropylacrylamide)-2-aminoethylmethacrylate hydrochloride
TC	Thermochromic
TIM	Transparent Insulation Materials
TT	Thermotropic
UDI	Useful Daylight Illuminance

polymer molecule aggregates due to a thermally-induced phase transition and its refractive index changes, resulting in a translucent appearance with high diffuse reflectivity [16,17]. This state attenuates a significant proportion of any incident solar energy and scatters the transmitted light, providing potential solar, glare and overheating protection. Early studies [18,19] investigated the optical properties of thermotropic layers in the scattering state through numerical simulation and experimental measurement [18]. Based on these studies, suggestions can be made to optimize the solar radiation switching performance of a thermotropic layer. Work exploring the application of thermotropic layers to building façades and glazing to address overheating risk and improve building energy efficiency stretches back over two decades [20–22]. Using in-situ measurements and TRNSYS simulation under the climate of Freiburg, Germany, Geoga et al. [21] concluded that applying thermotropic glazing to a residential building can deliver reductions in overheating with a knock-on 9% energy saving compared to a reference case. They also suggested that, due to the view-preserving properties in its translucent state, thermotropic glazing is more suitable for application in windows or skylights where the obscured view in the switched state is acceptable and where diffuse lighting is desired. Raice et al. [22] investigated the performance of a thermotropic system integrated into a demonstration house through both measurement and TRNSYS simulation. They concluded that one of the major challenges that underpins the success of TT material's application to windows is to select a suitable transition temperature. The transition temperature of a thermotropic layer can be tuned by adding salts or cosolvents and varying the concentration of TT material [13,23,24]. Nishio et al. [23] investigated the effect of salt additives on the transition temperature of a hydroxypropyl cellulose (HPC) material and concluded that the transition temperature can be adjusted by a number of candidate salts. The effectiveness of the salt additives in varying transition temperature depends on chaotropic effects. The effect of a cosolvent has been demonstrated by Wang et al. [24]. Their experimental results showed that glycerol is an effective additive capable of regulating the transition temperature of poly (N-isopropylacrylamide) (pNIPAm) hydrogels. Connelly et al. [13] demonstrated that increasing the concentration of a TT material can lead to a lower transition temperature. This effect is more obvious for aqueous solutions than membrane samples. The optical properties of TT materials also determine their effective application to windows. By

employing a manufacturing technique, such as changing TT material's concentration, particle size, or adding a cosolvent or cross linking compound, transmittance and diffuse reflection in its clear and translucent states can be adapted to suit building demands [13,24–26]. Resch et al. [27] found that the optical properties of TT films in their clear and scattering states were significantly dependent on the differences in the refractive indices of the components, additive content and distribution, as well as on the size of scattering domain. Connelly et al. [13] investigated the optical performance of a membrane containing various concentrations of HPC (e.g. 2, 4 and 6 wt% HPC). They concluded that increasing HPC concentration in membrane samples results in a lower transition temperature and a reduction in transmittance above the transition temperature due to the effect of increased HPC inter- and intrachain hydrophobicity. Wang et al. [24] illustrated that more cross-linking will reduce the material's transmittance before switching. Li et al. [25] researched the effect of particle size on the optical properties of a TT poly (N-isopropylacrylamide)-2-aminoethylmethacrylate hydrochloride (pNIPAm-AEMA) hydrogel material. Their results showed that by tailoring the particle size and internal structure, the difference in solar transmittance between clear and translucent states can be improved to 81.3%. Based on a 0.8 mm thick hydrogel layer formed between 4-mm thick glass plates with 2.7% volume fraction of particles, Maiorov [26] observed that with an increase in the average size of particles, the fraction of solar radiation scattered in the backward direction rapidly increases, reaching a well-defined maximum when the average diameter of the particles was 300 nm. However, it was noted that applying a TT material to the windows of a building would obstruct the building occupants' view during switching and in the switched state.

The integration of Transparent Insulation Material (TIM) into the windows of a building can improve the thermal resistance of window unit while facilitating more effective transmission of light. The use of TIM in solar collectors to suppress convective heat transfer can be traced back to 1960s [28–30]. Since then, experimental and theoretical studies have been conducted to investigate the thermal [31–36] and optical properties [37–41] of TIMs to improve their efficiency when applied to solar collectors, solar walls and glazing systems. Hollands et al. [42] presented their method for manufacturing a thin-walled (about 20  $\mu\text{m}$  wall thickness), large-celled (about 10 mm hydraulic cell diameter) honeycomb TIM from fluorinated ethylene propylene plastic, as well as their measurements of the honeycomb's thermal conductance and solar transmittance. They declared that if the cells cannot provide sufficient radiant suppression, it may be used in conjunction with low emissivity surfaces at one or both of its bounding faces. A polymer film based, small-celled TIM has been investigated by Wallner et al. [43,44] to explore the physical relationships between the material structure and the solar and infrared optical properties through theoretical model calculations. Their practical experience of applying 30  $\text{m}^2$  of this TIM system to the south facing wall of well insulated test house showed a solar energy efficiency of 44%, U-value of 0.76  $\text{W}/\text{m}^2 \text{K}$  and heat fluxes of up to 50  $\text{W}/\text{m}^2$  on cold sunny days can be achieved [45]. Our previous research [46–48] investigated the potential of applying a window integrated PS-TIM system in buildings to offer improvement in building energy efficiency and quality of the luminous environment. For window application, TIM performance is determined by its geometric configuration (e.g. slat spacing, honeycomb cell aspect ratio, etc.) and material characteristics (e.g. solar and daylight transmittance, thermal conductivity, emissivity etc.) [49–51]. PS-TIMs with translucent slats offer better performance in terms of daylight availability and uniformity as compared with PS-TIMs with transparent slats [47]. However, the presence of translucent slats reduces the desirable passive solar heat gains during heating period. Similarly, less daylight is transmitted into the room when the sky luminance is low, leading to additional lighting demand and energy consumption. The presence of translucent slats also limits and disturbs the occupant view to the external environment.

To address these shortcomings, a novel window system that incorporates PS-TIM and a TT material is studied in this paper. The PS-TIM

structure, which is located within the air cavity of a doubled-glazed window unit, aims to provide extra thermal resistance and effective daylight distribution. The TT membrane layer, which is encapsulated within the slat, aims to provide automatic daylight and solar regulation. The clear state of the TT PS-TIM window maximises solar and daylight admission, and maintains external views. In its translucent state, the TT PS-TIM system provides protection from overheating and oversupply of daylight while also retaining a proportion of the external view. Understanding how best to apply this novel window system, raises a number of questions around the features it should possess. This study explores the effects of geometry (i.e. slat spacing and slat tilt angle) and thermotropic features (i.e. transition temperature and optical properties) of the TT PS-TIM window system on building performance. A comprehensive methodology, which links the thermal and optical models for novel window system, with a building simulation engine for predicting energy performance and indoor luminous environment evaluation, has been developed to explore and optimize the design of TT PS-TIM system, providing an in-depth understanding of the system's performance. Although the investigated TT PS-TIM system is at the early conceptual stage, the results of this research offer initial guidance on the development of this novel window system for application in buildings and suggest significant potential for commercialization.

## 2. Thermotropic Parallel Slats Transparent Insulation Material (TT PS-TIM) window system

In this research, a cellular office space is used as a case study to explore the implementation of TT PS-TIM integrated into a double glazed window unit. A comprehensive workflow (Fig. 1) including thermal and optical characterisation and daylight and building energy simulation (i.e. EnergyPlus and RADIANCE) was used to explore how the PS-TIM's configuration and TT material properties affect the office energy and daylight performance. In the first phase, Computational Fluid Dynamics (CFD) software (FLUENT) was used to model the window unit's thermal properties and calculate its thermal conductance under different temperature scenarios. In the second phase, the PS-TIM structure with the thermotropic material in both its clear and translucent states were modelled using the genBSDF function in RADIANCE. This generates a Bidirectional Scattering Distribution Function (BSDF), which provides an optical description of the window unit. In the third phase, the dynamic thermal properties obtained from Phase 1 and the BSDF datasets obtained from Phase 2 were input into EnergyPlus for building energy simulation. In the fourth phase, an hourly profile showing the state of thermotropic layers (from which the clear state or translucent state BSDF was selected) was generated for use in RADIANCE to generate an annual daylight simulation.

### 2.1. Configurations of TT PS-TIM window systems

As shown in Fig. 2, the window unit comprised two 4 mm-thick float glass panes separated by a 15 mm air cavity to represent a typical double-glazed window design. Thermotropic parallel slats were located in and occupied the full width of the air cavity. There were no surface coatings applied to the glazing or the slats in what was an early prototype design. Each slat comprised a 0.5 mm thermotropic membrane sandwiched between two 0.25 mm Polymethylmethacrylate (PMMA) sheets (Fig. 2 (b)). The thermal conductivity of the PMMA sheets was 0.15 (W/mK) while the emissivity of its surfaces was 0.65. As this paper is investigating which geometric and thermotropic features of TT PS-TIM are most desirable for building application, different configurations in terms of slat spacing and slat tilt angle, and different transition temperature and optical properties were investigated and are described in this section.

As shown in the schematic diagrams in Fig. 3, the first group of windows explore 3 different slat spacings (10 mm, 7.5 mm and 5 mm) with all the slats placed horizontally and perpendicular to the glass panes (Fig. 3(a)). The second group explores 6 different slat orientation angles (30°, 45°, 60°, -30°, -45° and -60°) with a fixed slat spacing of 10 mm (Fig. 3(b)). For each configuration, slats with various thermotropic features (i.e. optical properties and transition temperature) were considered in the research.

Both the transition temperature and optical properties of a TT material can be adjusted through the use of salt additives, cosolvents or a cross linker, and by varying the concentration or particle size of TT material itself. Numerical modelling was used to identify properties that suit the application of a TT material to the PS-TIM window system. This offers an economic approach to understanding the desired behaviours of the TT layer to improve building energy demand and daylight quality, and then feed this back into the process of material design.

Candidate materials with 4 assumed optical transmission values (i.e. 10%, 20%, 30% and 40% in their translucent state) and 7 transition temperatures (19 °C, 21 °C, 23 °C, 25 °C, 27 °C, 29 °C and 31 °C) were assumed in the modelling. The TT membrane was assumed to have high visible transmittance (i.e. approx. 85%) in its clear state at temperatures below its transition temperature. The transmittance, reflectance and absorbance of the 4 materials after switching to their translucent state are shown in Table 1. These values were used in the numerical simulation to explore their effect on building energy demand and daylight quality.

The optical properties are based on measurements made on samples of HPC membrane performed at the University of Nottingham. To perform the measurement, a test slat with HPC membrane was mounted in a small temperature-controlled chamber with connections to a collimated light source and integrating sphere. The light illuminated perpendicularly on the sample at various temperatures and transmitted into the port of a transmittance integrating sphere, which collects the

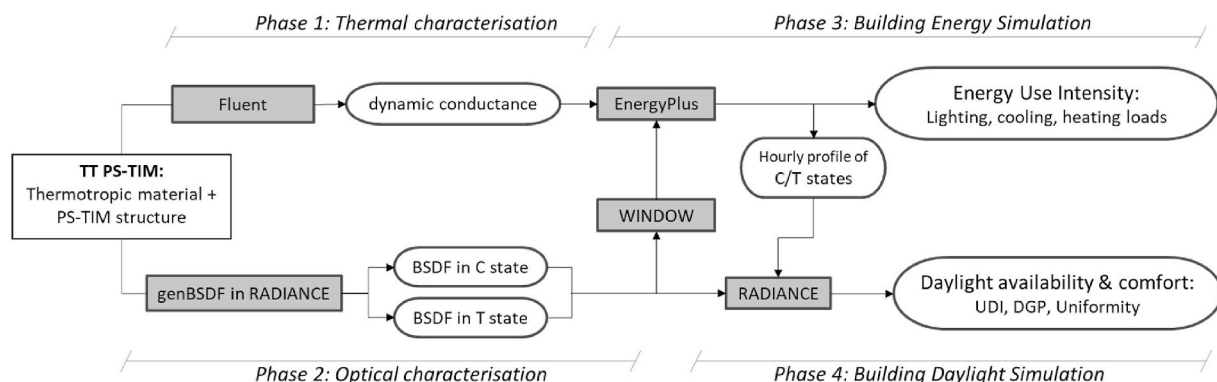


Fig. 1. Flow chart of the workflow for modelling TT PS-TIM window unit.

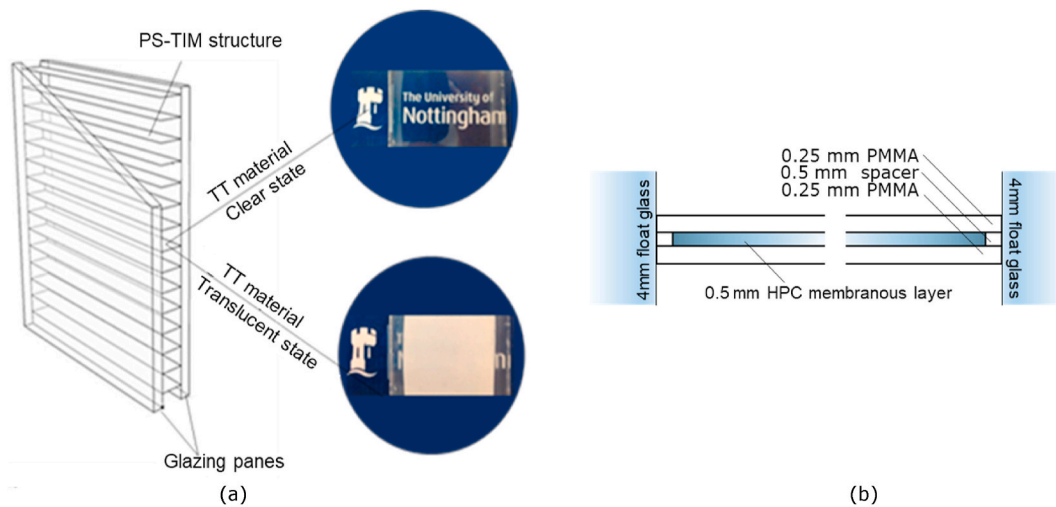


Fig. 2. (a) Schematic diagram of the window prototype with TT PS-TIM; (b) Schematic cross-section of a slat (not to scale).

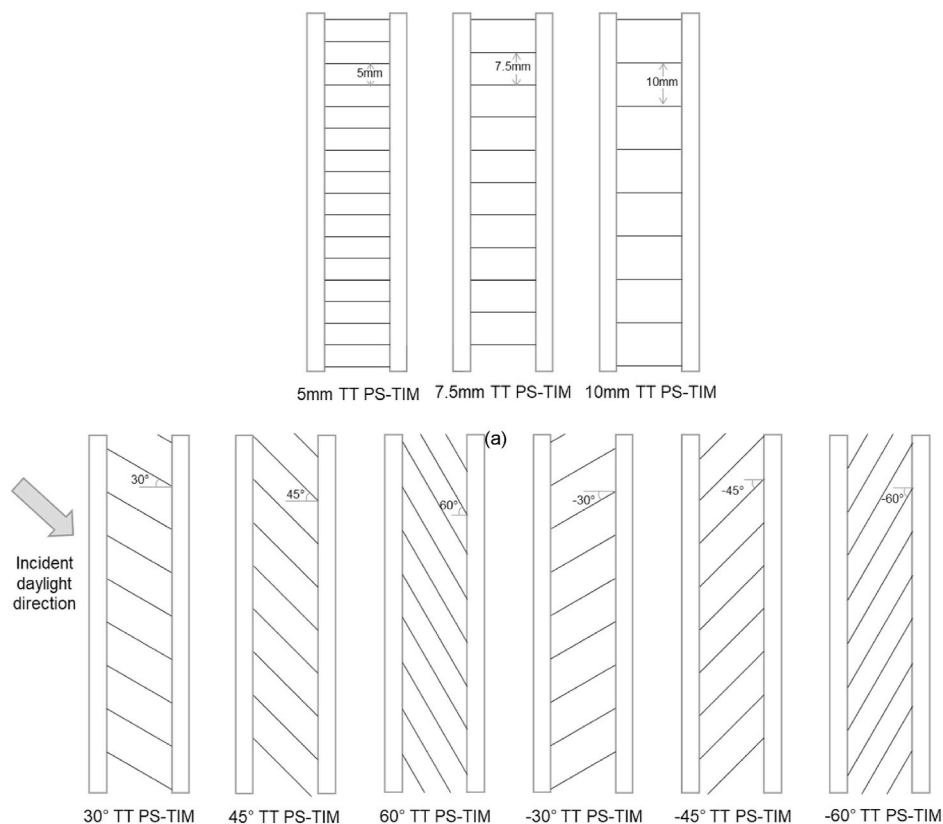


Fig. 3. (a) Cross-sectional view of PS-TIMs with various slat spacings; (b) Cross-sectional view of PS-TIMs with various tilt angles.

**Table 1**  
Optical properties of the thermotropic layers in their translucent state.

	Transmittance	Reflectance	Absorptance
TT PS-TIM (t 10%)	10%	35%	55%
TT PS-TIM (t 20%)	20%	35%	45%
TT PS-TIM (t 30%)	30%	35%	35%
TT PS-TIM (t 40%)	40%	35%	25%

light and quantified using a spectrometer to generate spectral transmittance for sample at various temperatures. Details of the measurement process can be found in Refs. [13,52]. Fig. 4 shows an example of the

measured data for a sample of HPC membrane indicating the variation in transmittance with temperature along with the change in its visual appearance.

It may be seen from Fig. 4 that the solar transmittance is similar in value to the visual transmittance: it was therefore assumed in the subsequent simulations that both could be approximated by the same transmittance, reflectance and absorptance values. There is no evidence of hysteresis present in the optical properties observed during heating-cooling cycles of pure HPC membrane samples [53], while a difference of about 0.5–1 °C in switching temperature between heating and cooling process has been observed after adding NaCl. Given its relatively small size, the difference in switching temperature evident in the

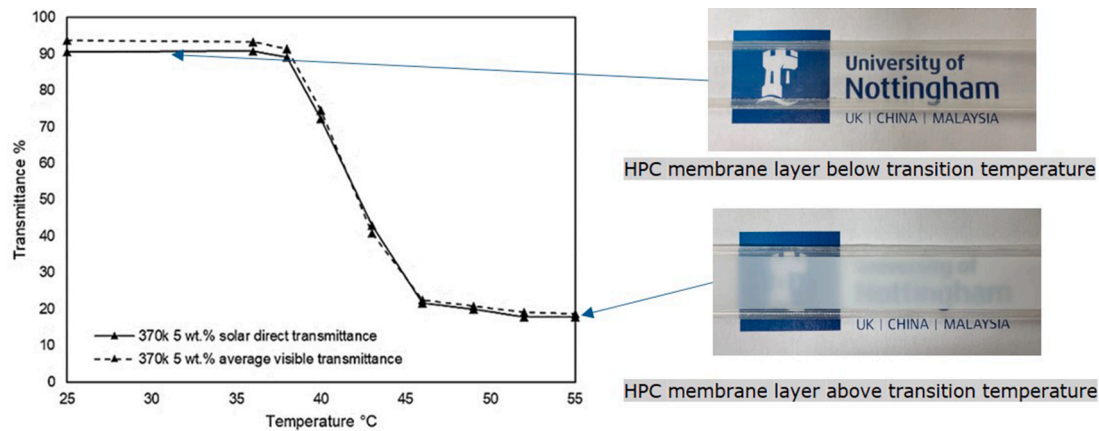


Fig. 4. Transmittance of HPC membrane with 370k Mw and 5 wt% with pictures of the HPC membrane layer below and above transition temperature.

heating-cooling cycle is neglected to simplify the subsequent simulation.

## 2.2. Optical and thermal characterisation of TT PS-TIM window systems

The geometry of the TT PS-TIM window systems shown in Fig. 3 was modelled in RADIANCE (v 5.1). Each was then optically characterised in both its clear and translucent state through the generation of a BSDF using the ray-tracing program embodied within RADIANCE - genBSDF. The RADIANCE dielectric material was used to model the glass [54] and the trans material, which provides the ability to model diffuse transmission [54], was used to model the TT layers integrated into the slats when in their switched states.

The generated BSDF files define coefficients to allocate light from each exterior direction to each interior direction. The BSDF data are based on Klems angle basis [55], which has been validated by McNeil et al. [55,56]. A key reason for selecting the Klem's method is its ability to create BSDFs for complex interstitial layers combined with glazing layers, and its compatibility with the software program WINDOW, which can be subsequently used in EnergyPlus as indicated in the workflow shown in Fig. 1. The resultant directional transmittance from the RADIANCE genBSDF simulation was compared with the results obtained from a TracePro virtual goniophotometer, following the BSDF validation methods reported in Refs. [57–59]. No significant difference exists between them.

Fig. 5 offers a sample BSDF for a single incidence angle (Altitude angle  $30^\circ$ , Azimuth angle  $0^\circ$ ) from the incoming hemisphere (highlighted in Fig. 5 (a)), to demonstrate the angularly resolved transmission for the different configurations of TT PS-TIMs, each assumed to be in its switched state with a transmittance of 40%. As can be seen in Fig. 5(b) for the double-glazed (DG) unit without parallel slats, incident daylight rays are not scattered. For the TT PS-TIM with horizontally placed slats at different slat spacing (Fig. 5(c)–(e)), increasing the spacing allows more of the scattered daylight to pass through the unit and produce a homogeneous distribution across the receiving hemisphere. For the window with slats tilted at  $30^\circ$  in Fig. 5(f), because the altitude angle of the incident rays ( $30^\circ$ ) matches the slat tilt angle, light is transmitted between the slats without significant scattering, behaving very much like the DG unit. As shown in Fig. 5(g), increasing the tilt angle to  $45^\circ$  means a proportion of the incident rays are incident on the slats and are diffused, this effect increasing with increasing tilt angle (Fig. 5(h)). When the slats are tilted at an angle of  $-30^\circ$ , all of the light is incident on the slats and the subsequent diffusion results in a well scattered distribution as shown in Fig. 5(i). For the more extreme tilt angles of  $-45^\circ$  and  $-60^\circ$  in Fig. 5(j) and (k) respectively, much of the transmitted light must pass through more than one slat, reducing the intensity on the receiving hemisphere.

To transfer the BSDF data into a unified file and subsequently import

it into EnergyPlus, the WINDOW (v 7.4) utility was used. As mentioned in section 2.2, to simplify the calculation, the TT material transmittance, reflectance and absorptance over the solar spectrum was assumed to be the same as that over the visible spectrum. Thus, the input transmittance and reflectance for TT slats in genBSDF over the visible spectrum was also used to define the transmittance and reflectance over the solar spectrum [55]. During the process of WINDOW modelling, the interstitial layer (i.e. all the parallel slats between two glazing panes and the space between them) was treated as a proxy component represented using the BSDF datasets and combined with the outer and inner glazing panes. This means those slats with high solar absorptance will absorb more solar energy than those with lower absorptance, leading to higher unit temperature and more hours where the TT membrane has switched to its translucent state. While the slats are treated as a whole component and the thermal state of this component was used to determine the switch state of the slats, the consequent heat transfer between slats resulting from absorption was not considered in this study. This is likely to have an insignificant effect on the annual energy performance, due to the minor temperature differences between individual slats and the equalising effect that convective and radiative heat transfer between slats would have on the whole.

For the thermal characterisation, the one-dimensional heat transfer equation for glazing systems embedded in EnergyPlus is inadequate for representing the thermal resistance of the proposed TT PS-TIM window system due to its complex structure. Therefore, a CFD model run on ANSYS FLUENT 15.0 was used to investigate the conductive, convective and radiative heat transfer properties of the proposed window unit, generating data that could be used in EnergyPlus for building simulation. The modelling method was validated through comparison of the simulation results with experimental data obtained from a series of tests conducted in a large climatic chamber (TAS Series 3 LTCL600) at the University of Nottingham, UK. The CFD simulation and experimental measurements show reasonable agreement with differences of less than 1% [60,61]. In the CFD model, the internal surfaces of the left and right glazing panes were set as two isothermal walls while the top and bottom ends were assumed to be adiabatic. The enclosure was filled with air ( $Pr = 0.71$ ). The fluid density and viscosity varied with temperature, while the remaining thermophysical properties of the fluid were assumed to be constant. The boundary conditions of the two isothermal surfaces were set to match 55 temperature scenarios (where the mean temperature of the two glazing panes ranged from  $-15^\circ\text{C}$  to  $35^\circ\text{C}$ , and the temperature difference between the two glazing panes ranged from 5K to 25K) representing the commonly encountered conditions experienced in the built environment. The thermal performance predicted under each of these 55 temperature scenarios was then converted into an equivalent thermal conductivity for the proxy component, representing the combined convective and radiative heat transfer through the complex structure

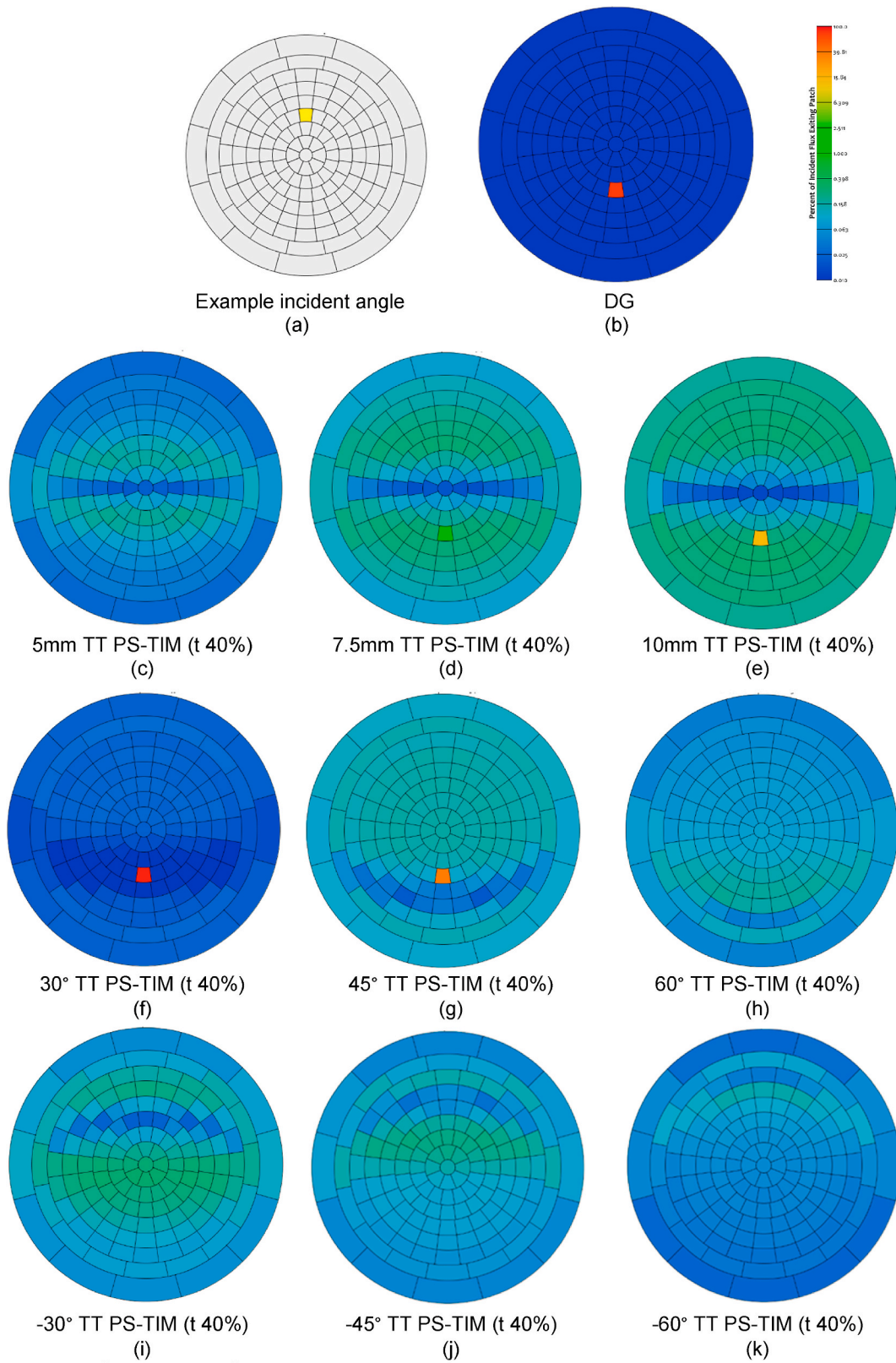


Fig. 5. BSDFs of the TT PS-TIM window unit with different optical properties: an example of one incident angle (Altitude angle 30°, Azimuth angle 0°).

within the glazing unit. A series of individual values of equivalent thermal conductivity employed in EnergyPlus was then used to represent the dynamic thermal conductivity of the complex window system in building simulation studies of annual performance [46]. An example of the equivalent thermal conductivities for the 10 mm TT PS-TIM

structure under these 55 temperature scenarios is given in Fig. 6.

### 3. Building simulation methodology

Once the TT PS-TIM glazing had been characterised thermally and

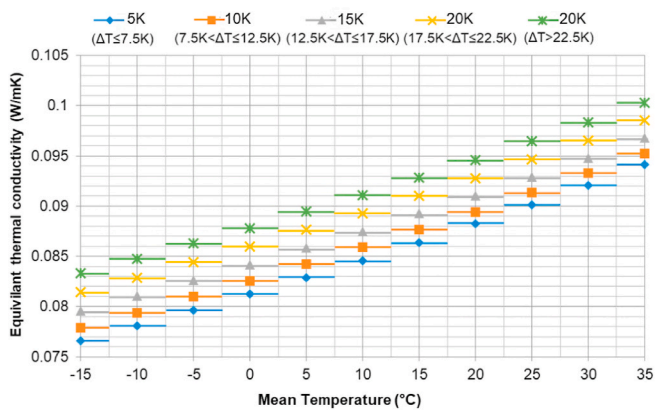


Fig. 6. Equivalent thermal conductivities for 10 mm TT PS-TIM window (slat tilt angle 0°) under 55 temperature scenarios.

optically, building energy and daylight simulation packages were used to predict the effect of the glazing on building performance.

### 3.1. Energy simulation through EnergyPlus

As illustrated in Fig. 7, a cellular office with dimensions 2.9 m (width) × 4.4 m (depth) × 3.3 m (height), which was assumed to form part of a large office building, was selected and studied in EnergyPlus to evaluate how the various geometric configurations and thermotropic features of the TT PS-TIM glazing influenced building energy performance. The design of this simulated space is based on a real office in the Energy Technologies Building at the University of Nottingham, UK. EnergyPlus itself has been developed and validated according to the American Society of Heating, Refrigerating and Air-Conditioning Engineers (ASHRAE) Standards using measured data obtained from relevant test facilities [62]. To develop confidence in using EnergyPlus for evaluating building performance of a room served by a smart window system, the modelling method was verified through comparison of simulation results with the measured data. More details of this procedure can be found in the authors' previous publication [63]. In this paper,

a window of dimensions 1.4 m (height) × 2.9 m (width) was located in the single exposed wall of the office, which was assumed to be oriented towards the equator. The remaining room surfaces were assumed to be buffered by mechanically conditioned spaces, represented using adiabatic boundaries. One hour time steps run for an entire year using the International Weather for Energy Calculation (IWEC) weather data for London were used as the input for the building simulation. Influences from surrounding buildings, vegetation or other obstructions were ignored. The office was assumed to be occupied by two people from 09:00 to 17:00 on weekdays. Standard equipment and lighting loads of 13 W/m<sup>2</sup> and 16 W/m<sup>2</sup> respectively were used for the study following the guidance from Chartered Institution of Building Services Engineers (CIBSE) and Part L2 during occupancy hours [64,65]. The thermostat set point temperature for heating and cooling determined the room temperature when a heating, ventilation, and air conditioning (HVAC) system is included in the model. This affects the window temperature and thus the TT material's clear and translucent states. The thermostat setting temperature and TT material state will then influence the resultant office heating and cooling energy consumption. To simplify the analysis, set points of 25 °C for cooling and 21 °C for heating were assumed during office hours but beyond this, the influence of thermostat set point on the office energy consumption is not discussed in this study.

The BSDF datasets for the TT PS-TIM window system in its clear and translucent states were exported to EnergyPlus. The equivalent thermal conductivities of the interstitial layer under the 55 temperature scenarios obtained from FLUENT were also input into EnergyPlus. During the annual simulation, the built-in 'Energy Management System (EMS)' function was used to determine when switching occurred between the clear and translucent states of the TT material, as well as the equivalent thermal conductivities of the interstitial layer. To do this, virtual sensors were used to monitor the temperatures of the interstitial layer and glazing panes, and based on the detected temperatures at the beginning of each time-step in the building simulation, the state of TT material and the thermal conductivity of the glazing unit were determined. If the temperature of the interstitial layer was below the thermotropic transition temperature, BSDF files for the clear state were applied in the subsequent energy balance calculation, otherwise the BSDF files for the window in its translucent state were applied. Similarly, based on the

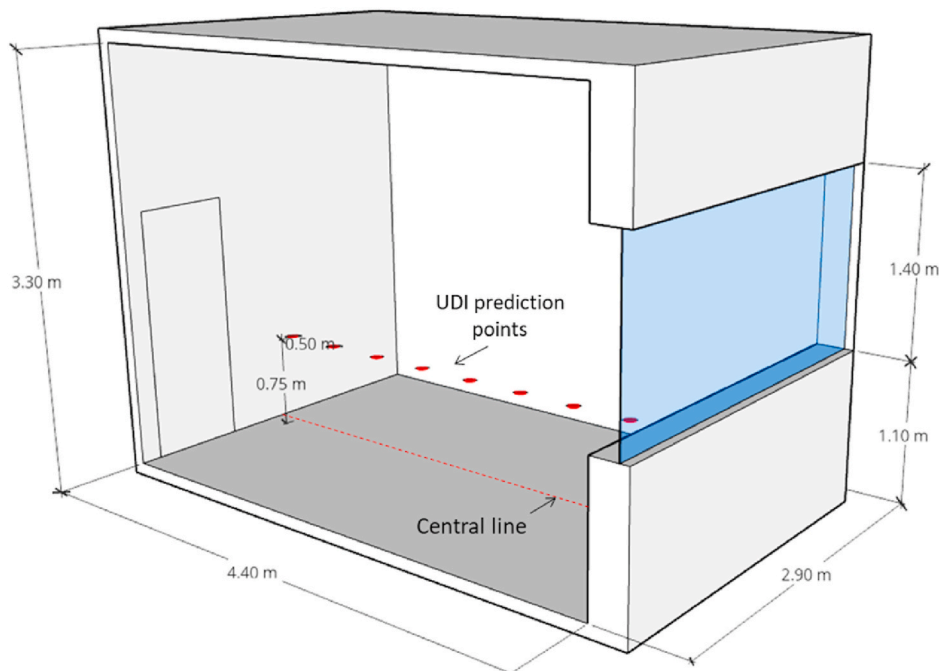


Fig. 7. Sectional view of the office and the positions selected for evaluating illuminance distribution.

mean temperature of the two glazing panes and the temperature difference between them at the beginning of each time-step, the corresponding thermal conductivity of the interstitial layer was selected for energy balance calculation. For example, for the 10 mm TT PS-TIM unit (slat tilt angle  $0^\circ$ ), if the mean temperature of the two glazing panes was between  $7.5^\circ\text{C}$  and  $12.5^\circ\text{C}$  and the temperature difference between them was less than  $7.5\text{K}$ , a thermal conductivity of  $0.085\text{ W/mK}$  was used in the energy balance calculation at the corresponding time-step. Once the EnergyPlus simulation was completed, an hourly profile showing the thermotropic material's state at each time step was generated and used subsequently in RADIANCE for annual daylight prediction.

### 3.2. Daylight simulation through RADIANCE

The three-phase method in RADIANCE, which provides an accurate and time-efficient way to conduct an annual daylight simulation, was applied in this study [66]. The RADIANCE model of the office has been validated through comparison of simulation results of illuminance at several points in the simulated room with experimental measurements taken in the real office under the same conditions. The results agree reasonably well with most of the points tested showing deviations no greater than 3.6%. The greatest deviation, in the order of 13%, occurred at points 0.5 m away from the window and are due to slight geometry differences between the model and the real office [47]. More details about the RADIANCE modelling and validation can be found in the authors' previous publication [47]. The following expression:

$$I = VTDS$$

was used to calculate the illuminance or luminance,  $I$ , at the points of interest inside the room for a time series. Nine points located along the central line of the office from window to the end wall with 0.5 m interval distance were selected to represent the Useful Daylight Illuminance (UDI) distribution on a working plane positioned at a height of 0.75 m above floor level as illustrated in Fig. 7. Here,  $V$  is the view matrix and  $D$  is the daylight matrix, describing the external and internal conditions respectively. The sky matrix,  $S$ , is a time series of sky vectors, which is generated by dividing the whole sky into discrete patches, with each patch being assigned an average radiance value for a given time and sky condition. The transmission matrix,  $T$ , characterizes flux output as a function of input for a particular configuration, represented in the BSDF [67,68]. In this study, instead of using a single set of transmittances for the window materials, 2 matrices were used to represent the thermotropic material: one for its clear state and one for its translucent state. The appropriate state (transparent or translucent) was determined from the hourly schedule file output from the EnergyPlus calculation based on window temperature.

## 4. Results and discussion

### 4.1. TT PS-TIM windows with varying slat spacing

This section presents annual energy consumption and daylight availability of the prototype office when using TT PS-TIM window units with horizontal slats. The effect of the TT materials' optical properties and switching temperature on annual daylight and energy performance were analysed, and optimized designs proposed.

#### 4.1.1. The effect of slat spacing on energy and daylight performance

To investigate how the slat spacing affects the overall daylight and energy performance of the office room served by TT PS-TIM windows, units with a translucent-state transmittance of 40% and transition temperature of  $25^\circ\text{C}$  were studied. In order to explore the mechanism through which savings were made, the results were compared with simulations using a conventional double-glazed window, a window with

clear PS-TIM (i.e. slats with the same optical properties as the TT slats in their clear state- identified as C PS-TIM on the graphs that follow) and a window with translucent PS-TIM (i.e. slats with the same optical properties as the TT slats in their translucent state- identified as T PS-TIM on the graphs that follow). The energy consumption was divided into heating, cooling, and lighting demand. UDI [69] was used as the metric to explore occupant response to the luminous environment. The UDI was determined based on the predicted illuminance at the points distributed across an assumed working plane 0.75 m above floor level as indicated in Fig. 7. Illuminance values lower than 500 lux were assumed to represent insufficient daylight availability requiring the use of supplementary artificial lighting. Illuminance values higher than 2000 lux were assumed to represent an oversupply of daylight causing visual discomfort and a potential for glare. A useful UDI was therefore assumed to lie within the illuminance band between 500 lux and 2000 lux, where a typical office design illuminance is met.

As shown in Fig. 8, clear PS-TIM window systems offer annual energy savings when compared with a standard double-glazed window unit (with savings of between 4.5% and 5.8%). Translucent PS-TIM window units can provide larger annual energy savings (between 10.2% and 13.8% for the units with 7.5 mm and 10 mm slat spacing), however, care must be exercised as the window unit with 5 mm spacing results in an increase in energy consumption (of 5.4%) due to an increased demand for supplementary artificial lighting. Among all the tested window systems, the three TT PS-TIM window units provide the best overall energy saving potential under the selected London climate, varying from 16.5% to 20.9%. The majority of the energy saving results from significant reductions in cooling loads and slight reductions in heating load. The cooling energy saving is achieved because a significant proportion of undesirable solar heat gain is excluded by the TT PS-TIM system when ambient conditions are warm and it is in its translucent state. There is a small difference between the cooling loads for the 5 mm, 7.5 mm and 10 mm TT PS-TIM systems and overall they are significantly lower than those of conventional DG and PS-TIM systems. This demonstrates that the thermotropic layers work effectively for regulating undesired direct solar gain during cooling season. Increasing the slat spacing results in increased demand for cooling energy, this being a consequence of increased transmission due to the changing geometry. Savings in heating energy are achieved as a result of reduced heat loss from the window system because the presence of PS-TIM increases its thermal resistance and the TT layer admits beneficial solar gain. The heating load of the 3 TT PS-TIM systems was similar to that of the clear PS-TIMs, suggesting that the TT layers are in their clear state and so admitting beneficial solar gains during most of heating season. Although increased slat spacing increases the thermal transmittance of the TT PS-TIM window units, and so demand for heating energy, the effect is weak. Demand for lighting energy increases for all of the TT PS-TIM window units when compared to that for DG and the clear PS-TIM due to the reduced transmission of daylight when in its switched state. Comparison with the energy demand for window units containing translucent PS-TIM indicates that the switching offered by the TT layer offers benefits through reductions in lighting energy when compared with a strategy adopting permanently translucent TIM to offer protection from overheating.

Looking at the combined heating, cooling and lighting performance, the TT PS-TIM window units offer the lowest annual energy demands with the 7.5 mm TT PS-TIM (t 40%,  $25^\circ\text{C}$ ) window unit delivering the maximum saving of 20.9%. This stems largely from the balance between savings in lighting and cooling energy demand, the 5 mm TT PS-TIM (t 40%,  $25^\circ\text{C}$ ) offering lower cooling but higher lighting energy demand (delivering an overall 16.5% reduction in annual energy demand), and the 10 mm TT PS-TIM (t 40%,  $25^\circ\text{C}$ ) offering lower lighting but higher cooling energy demand (delivering an overall 19.9% reduction in annual energy demand).

Fig. 9 presents the useful UDI distributions taken along the central line of the office when served by the TT PS-TIM with horizontal slats, as well as the DG, Clear PS-TIM, and Translucent PS-TIM window units.

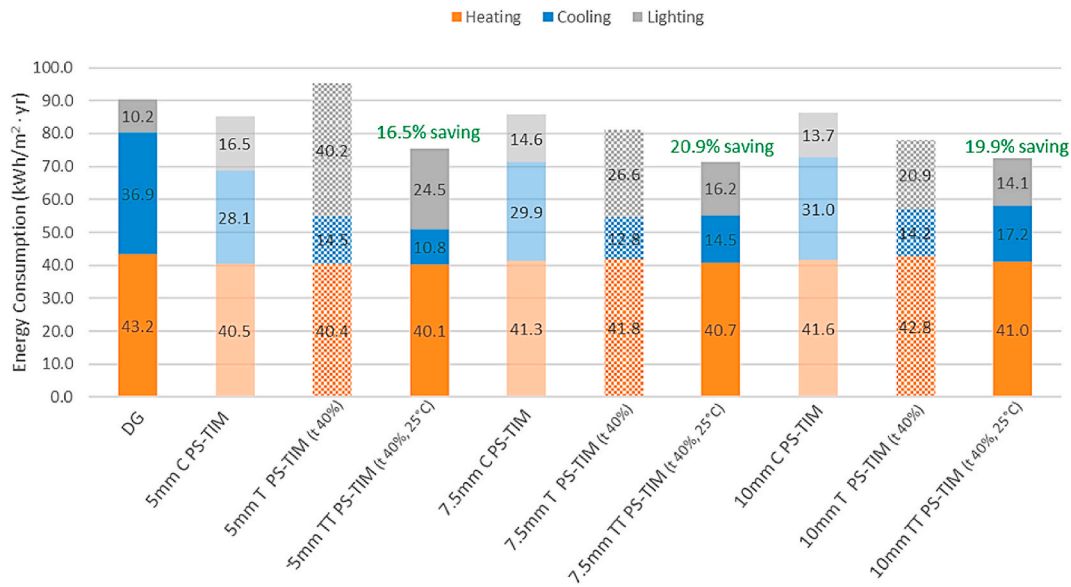


Fig. 8. Annual heating, cooling and lighting energy demand for a cellular office served by a TT PS-TIM window with different slat spacing for a slat tilt angle of 0°.

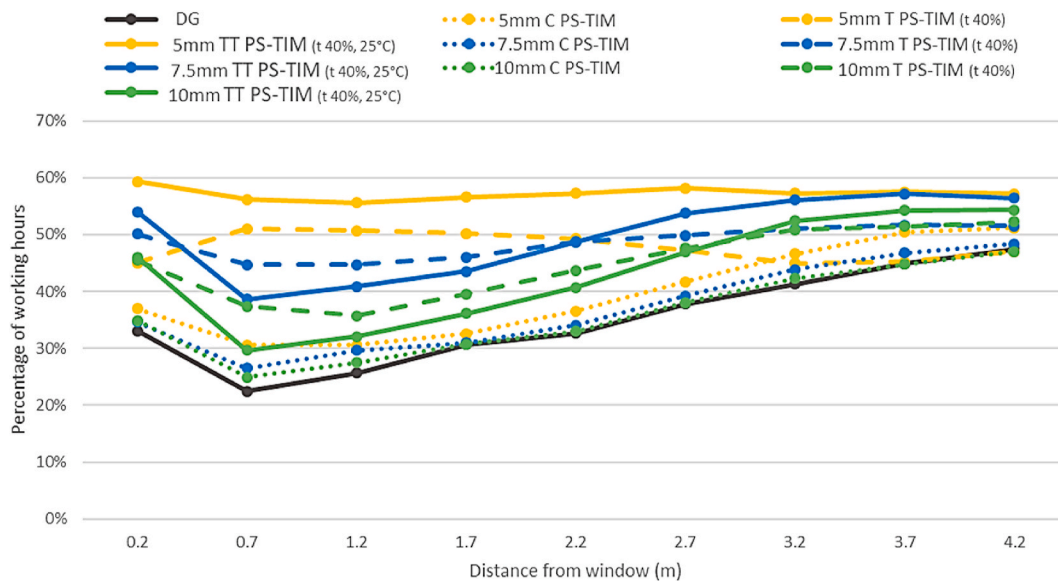


Fig. 9. UDI<sub>500–2000 lux</sub> distribution in the office for TT PS-TIM systems with different slat spacing for a slat tilt angle of 0°.

The UDI for the DG window varies between 22% and 47%. The region that is close to the window shows the lowest UDI of all the window combinations, mainly because of a high incidence of over illumination, i. e. periods when the illuminance exceeds 2000 lux account for 45%–65% of working hours at locations within 2.2 m of the window. The use of the clear PS-TIM windows slightly increase useful daylight availability (i.e. 500 lux < UDI < 2000 lux) by reducing the oversupply of daylight in the area near the window when compared with the DG window. The translucent PS-TIM can effectively scatter daylight and significantly reduces the oversupply of daylight near the window, improving the daylighting quality of the room. However, it also increases the under-supplied daylight hours due to the reduced transmittance of the translucent layer. For example, the 5 mm Translucent PS-TIM could improve the UDI<sub>500–2000 lux</sub> in the region within 2.2. m of the window to around 50%, but this comes at a cost, with the daylight availability for the deeper part of the room dropping to 45% due to its lower daylight transmittance. When the window temperature is over 25 °C (i.e. the transition temperature in this scenario), the TT PS-TIM windows switch

to their translucent state. This usually happens when the solar radiation is strong, which also means the presence of strong sky luminance, and the two in combination result in an effective reduction of daylight oversupply. When the sky luminance is low, the TT PS-TIM system is usually in its clear state, resulting in an unattenuated supply of daylight. The 5 mm TT PS-TIM provides the best daylight performance of all the window units investigated. The UDI lies in the range of 56–59% across the full depth of the room, indicating a homogeneous daylight distribution. The 7.5 mm and 10 mm TT PS-TIM provide similar average UDI when compared with their translucent PS-TIM counterpart, however, applying TT PS-TIM increases the daylight availability at the back of the office, in the region far away from the window.

#### 4.1.2. The effect of TT material optical properties on energy and daylight performance

This section explores the effect of the TT materials' optical properties (i.e. its translucent-state transmittance) on the building performance when it is applied to TT PS-TIM windows with different slat spacing. As

in the previous section, the transition temperature of the thermotropic layer was assumed to be 25 °C to exclude its influence on energy efficiency and daylight performance.

The demand for heating, cooling and artificial lighting energy are compared with the performance of a standard DG window in Fig. 10. All the TT PS-TIM windows deliver energy savings, the majority of which stem from significant reductions in cooling load. It may be seen that the 7.5 mm TT PS-TIM window offers an energy saving of between 14.3% and 20.9% under the selected London climate; and shows similar overall reductions to the 10 mm TT PS-TIM, which delivers overall energy savings of between 16.9% and 19.9%. The former has smaller cooling loads than lighting loads and for the latter, this pattern is reversed. Performance of the 5 mm TT PS-TIM is relatively poorer, and for the low transmittance cases (i.e. 10% and 20%), energy savings are less than 10%. For the three groups, there is a trend indicating that higher transmittance offers a higher energy savings. However, the results for the clear PS-TIM windows (i.e. without the TT layer, representing the limit when the TT PS-TIM has a transmittance of 85%) in Fig. 8 would suggest that there is an optimal value of transmittance, after which potential further reductions would deliver smaller energy savings.

Fig. 11 shows the distribution of useful UDI (UDI 500–2000 lux), used here to quantify the daylight performance of the office served by the TT PS-TIM windows. All the windows incorporating a TT layer offer improved performance over the DG window. The best performing is the 5 mm TT PS-TIM prototype, which for all values of transmittance, offer an even distribution of daylight throughout the room depth, especially in those regions 0.7 m–2.2 m from the window, showing differences of about 3%. For the transition temperature used in this scenario (i.e. 25 °C), the 7.5 mm TT PS-TIM windows with higher transmittance (i.e. 30% and 40%) and 10 mm TT PS-TIM windows with all the tested optical properties, while better than the DG window, fail to provide sufficient reduction in the oversupply of daylight, leading to lower daylight availability in the region away from the window. The general trend is that as the slat spacing grows wider and the transmittance approaches 100%, the daylight performance approaches that of the DG window, as would be expected.

#### 4.1.3. The effect of TT material transition temperature on energy and daylight performance

In this section, the transition temperature is varied between 19 °C and 31 °C with a 2 °C interval for each of the TT PS-TIM windows explored in section 4.1.2, where the optical transmittance was the key variable. The resulting performance is shown in Fig. 12, reported in terms of the overall energy savings achieved for each TT PS-TIM window when compared with the energy demand of the office served by the standard DG window.

As can be seen, 5 mm TT PS-TIM windows with a low transition temperature (i.e. 19 °C and 21 °C) and low transmittance perform worse than the DG window in terms of energy demand. Higher transition temperatures start to yield energy savings, these increasing with increasing transmittance. The optimal transition temperature within this group decreases with increasing transmittance.

For the two wider slat spacings, energy savings are significantly higher for all cases. Both the 7.5 mm TT PS-TIM and 10 mm TT PS-TIM windows offer their peak energy saving for a transmittance of 40%, the former at a transition temperature of 23 °C (delivering a 22% saving in energy) and the latter at 21 °C (delivering a 21.7% saving).

The results suggest that maximising energy savings involves achieving a balance between the slat spacing and the transmissivity of the slats, both of which affect the transmitted radiation. For the range of variables considered here, higher transmissivity offers larger energy savings. As the slat width is increased, lower transition temperatures, which imply more time is spent in the translucent state, are required to counter the increased transmission taking place between the slats.

Fig. 13 presents the useful UDI distribution taken along the centre line of the office for the TT PS-TIM windows with a transmittance of 40%. Illuminance predictions were made for transition temperatures varying from 19 °C–31 °C.

It may be seen that all of the 5 mm TT PS-TIM windows deliver a relatively uniform availability of useful light across the full depth of the office with an average UDI exceeding 50%. Lower transition temperatures, and hence more time spent in the translucent state, improve conditions close to the window, but result in fewer hours where suitable conditions occur at the rear of the office. Decreasing the transition temperature, and hence increasing the number of hours spent in the clear state, results in reduced useful UDI in the region next to the window but improved conditions at the rear of the office. For all of the window variants, the transition between these two zones appears to occur approximately 2.7 m from the window and the transition temperature that gives the best balance of conditions across the full room depth is 23 °C.

The 7.5 mm and 10 mm TT PS-TIM window variants all show a pattern of decreasing working hours with a useful UDI as transition temperature increases (and the window spends more time in its clear state), with the region next to the window showing the worst performance. This echoes the behaviour observed for the 5 mm TT PS-TIM, where the attenuation and diffusion of light by the slats in their switched state is beneficial, and highlights the effect of the slat spacing. As the spacing increases, direct transmission, bypassing the TT layer increases increasing oversupply of daylight in the region next to the window.

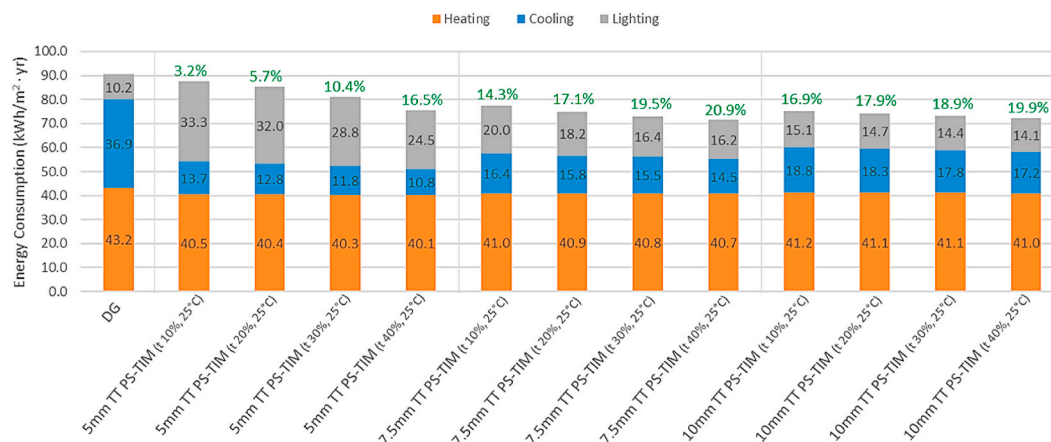


Fig. 10. Annual heating, cooling and lighting energy demand for TT PS-TIM systems with different slat spacing and a tilt angle of 0° - TT material transition temperature is 25 °C and its translucent state optical properties vary.

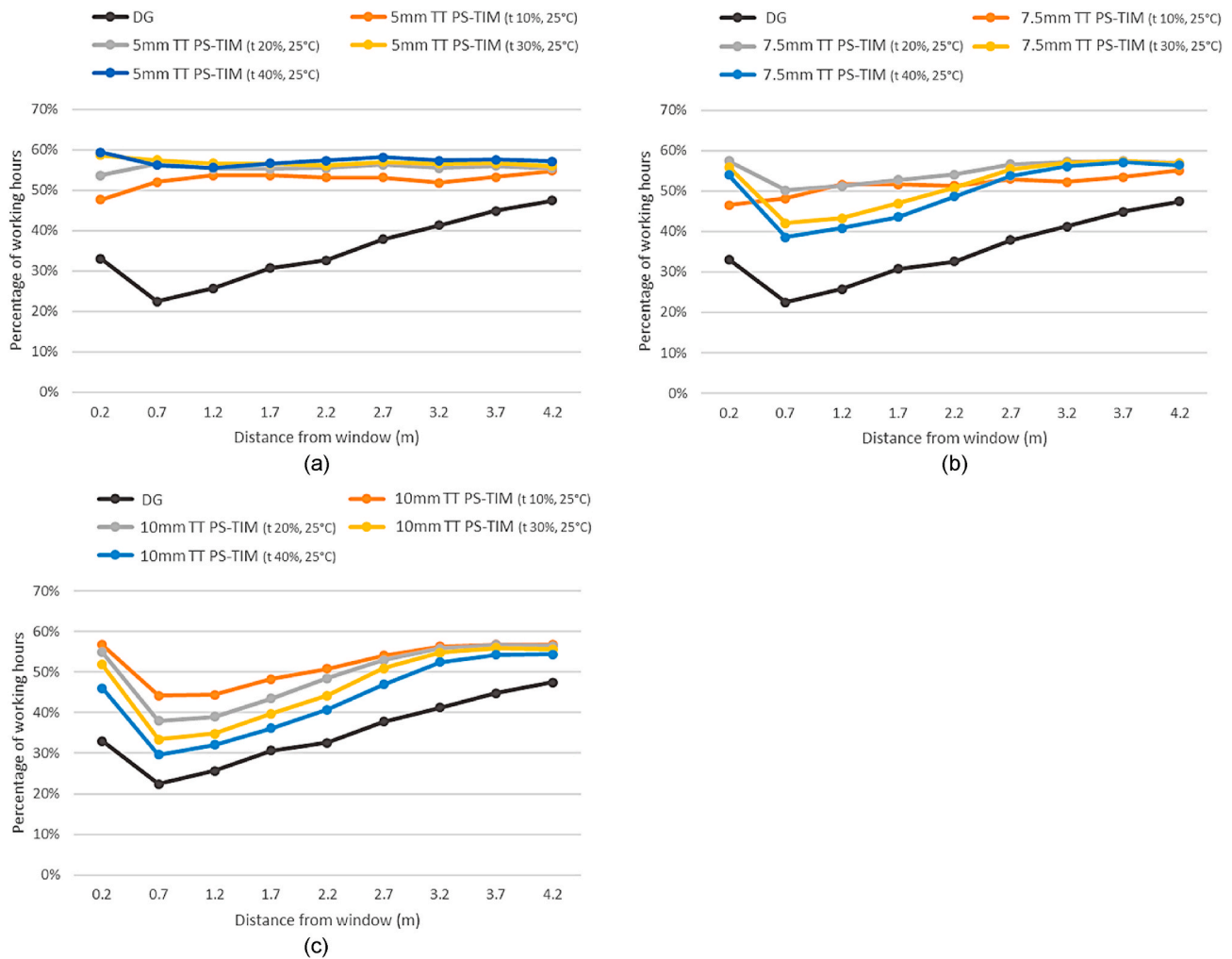


Fig. 11. UDI<sub>500-2000 lux</sub> distribution in the office for TT PS-TIM systems with different slat spacing and a tilt angle of 0° - TT material transition temperature is 25 °C and its translucent state optical properties vary.

4.1.4. Optimized design scenarios

An optimized design is achieved by comparing the energy saving potential and average UDI performance for the office space served by the TT PS-TIM windows with horizontal slats at 5 mm, 7.5 mm and 10 mm spacings under the range of variables investigated above as shown in Tables 2–4. Both the energy and daylight performance are classified into five bands: ‘best’ (dark green), ‘good’ (light green), ‘moderate’ (yellow), ‘poor’ (light red) and ‘worst’ (dark red). Designs that can provide best/good energy performance and simultaneously best/good daylight performance are adopted as the optimized design.

It may be seen that the 5 mm TT PS-TIM performs strongly with respect to daylight performance as quantified by UDI, especially for translucent states with transmittance of 20%, 30% and 40%, and transition temperatures between 21 and 25 °C. However, the energy efficiency of 5 mm TT PS-TIM systems for most of the TT material combinations tested is poor. It is worth noting that while daylight performance as quantified using UDI is strong, when quantified using energy, it is relatively poor – in its low transmittance states (i.e. 10% and 20%) there is insufficient daylight resulting in high demand for artificial lighting energy. This variant of the window therefore deals effectively with those hours when daylight is plentiful but less well when it is not.

The 10 mm TT PS-TIM shows the best energy saving potential provided the transition temperature is not too high, however, only specimens with a lower translucent-state transmittance (e.g. 10% and 20%) and a relatively low transition temperature (e.g. 19 °C and 21 °C) can provide good levels of daylight performance. The 7.5 mm TT PS-TIM

with translucent-state transmittance of 30% and 40% provide the greatest energy saving potential and simultaneously good levels of daylight availability if their transition temperature is in the range of 21–23 °C. The optimized designs of 10 mm and 7.5 mm TT PS-TIM are bold and underlined in Tables 3 and 4

As discussed in section 4.1.3 the results suggest a balance is struck between controlling solar gains, limiting over illumination of the space in the vicinity of the window, and delivering sufficient daylight to avoid the use of artificial lighting. Increasing the slat spacing increases the proportion of incident light that is transmitted directly into the space, and is therefore not controlled by the TT layer (this is evident for the 10 mm slat spacing). This tends to support the use of TT layers with lower transmissivity in their switched state (to offer greater attenuation of the light they intercept) and lower transition temperatures (so the TT layer spends more hours in its translucent state). For the closer slat spacing (7.5 mm), the TT layer controls a greater proportion of the incident light, favouring lower transmissivity and higher transition temperatures. The relatively close correlation of unwanted solar gains with high ambient light levels means that higher transition temperatures will help control overheating and simultaneously offer better levels of useful illumination in the office during the warmer parts of the year. During the colder parts of the year, when in their unswitched state, the TT layer will allow effective transmission of light when ambient light levels are lower, hence reducing the need for artificial lighting.

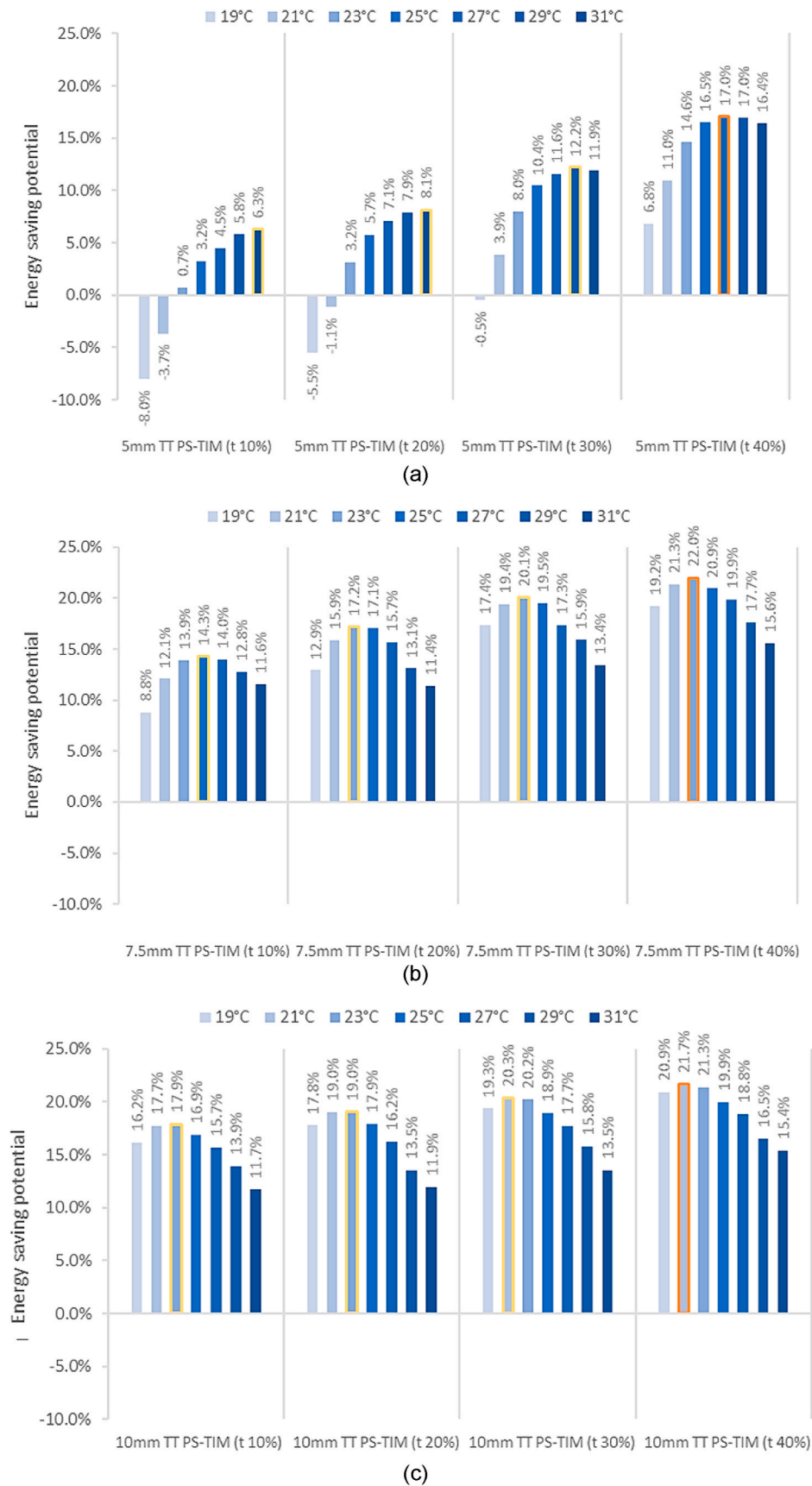
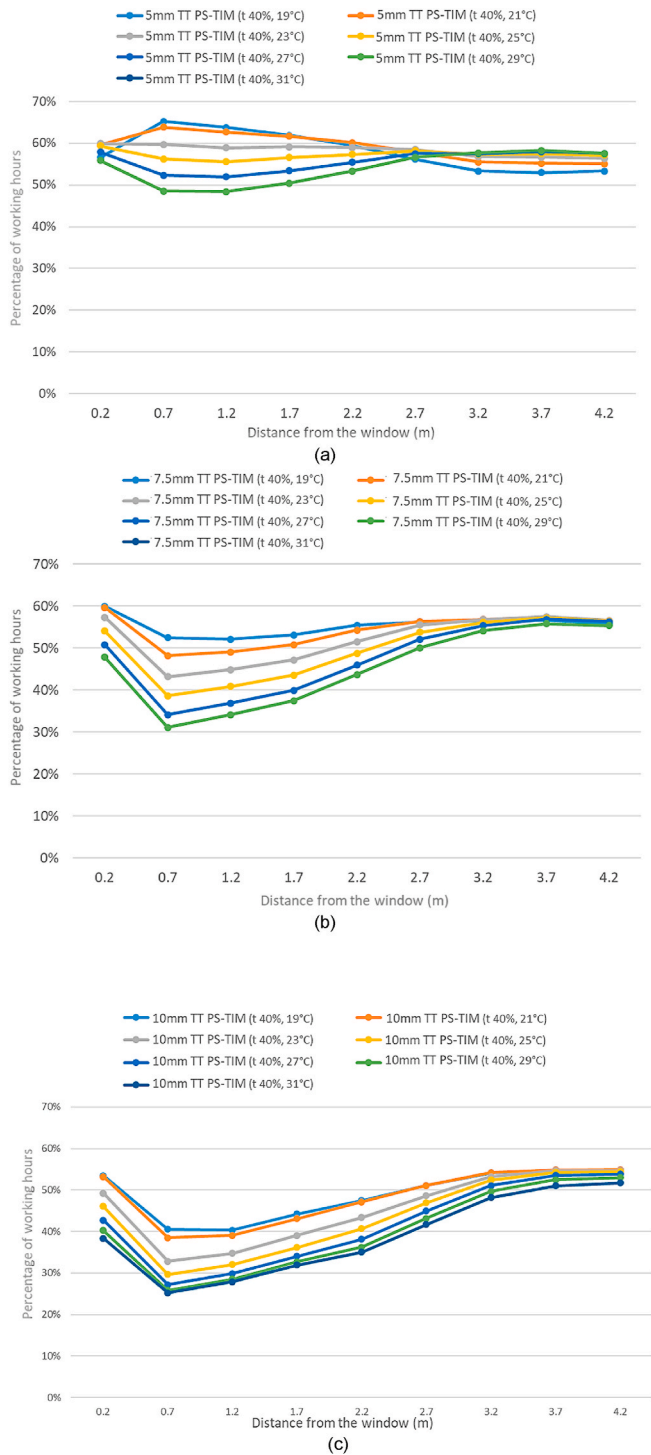


Fig. 12. Annual energy saving potential for TT PS-TIM systems with different slat spacing and a tilt angle of 0° - TT material transition temperature and translucent state optical properties vary.



**Fig. 13.** UDI<sub>500-2000lux</sub> distribution in the office for TT PS-TIM systems with different transition temperatures at (a) 5 mm slat spacing, (b) 7.5 mm slat spacing and (c) 10 mm slat spacing - tilt angle 0°, TT material optical properties in the translucent state are transmittance 40% and reflectance 35%.

#### 4.2. The effect of slat angle

This section reports the results for the predicted energy demand of the cellular office served by the TT PS-TIM windows with tilted slats as shown in Fig. 3(b). The slat spacing was kept constant at 10 mm as was the transmittance of TT material in its translucent state, which was assumed to be 40%. Data for the DG window and for the TT PS-TIM window with un-tilted slats are provided for comparison.

#### 4.2.1. The effect of slat angle on energy and daylight performance

Fig. 14 shows the variation of heating, cooling and lighting energy consumption for the TT PS-TIM at different tilt angles. The transition temperature of the thermotropic layer was assumed to be 25 °C in this section.

As can be seen, although all these TT PS-TIM windows demonstrate potential for energy saving when compared with the DG window, none of the designs provides a better energy saving potential than TT PS-TIM window with un-tilted slats.

Performance can be broadly divided into 2 categories – those designs with their slats tilted towards the sky vault (i.e. the designs with positive tilt angles, allowing some of the incident to bypass the TT layer) and those with their slats tilted towards the ground (i.e. those designs with negative tilt angles where most of the incident radiation is incident on the TT layer). Designs with positive tilt angles deliver more daylight but admit more solar gain, reducing demand for supplementary artificial lighting but increasing cooling energy demand. As the tilt angle increases, the slats screen each other and the view factor becomes smaller, meaning that much of the diffused light has to pass through further slats to enter the room. This reduces solar gain and light levels, thus reducing cooling loads and increasing demand for lighting energy. Slats with negative tilt angles show the same pattern of behaviour with increasing tilt angle but because most of the radiation passes through the TT layer, they offer greater reductions in cooling energy demand offset against greater demand for supplementary artificial lighting. This results in higher total demands for energy as compared with their counterparts with positive tilt angles.

The results for daylight availability as quantified using UDI, in Fig. 15, indicate that the performance of the TT PS-TIM windows varies between the front and rear of the office.

At the front of the office, next to the window, useful UDI hours for the DG window are low due to over illumination. Those windows with their slats tilted towards the sky vault (ie 30°, 45° and 60°) allow the direct transmission of some of the incident radiation resulting in over illumination. Those windows with their slats tilted away from the sky vault (ie -30°, -45° and -60°) show increasing hours of useful illumination as most of the incident radiation is intercepted by the TT layer, and as the tilt angle increases, a greater proportion must pass through more than 1 TT layer.

The rear of the office receives less light, and for those windows where transmission through more than 1 slat is occurs (i.e. 60° and -60°), useful daylight levels are low. The windows with slats tilted away from the sky vault at shallow tilt angles (i.e. -30°, -45°) avoid the direct transmission of light but allow sufficient transmission through the TT layer to provide good levels of illumination at the rear of the room. This pair offers the best balance of UDI<sub>500-2000lux</sub> hours across the full depth of the room, at 53% and 56% respectively.

#### 4.2.2. Transition temperature

Fig. 16 shows the total energy saving potential of the TT PS-TIM windows when compared with the DG window for simulations where the TT material transition temperature is varied between 19 °C and 31 °C. The transition temperature has the most significant effect on -45° and -60° tilt angles while it has the least effect on 30° TT PS-TIM. The optimal transition temperature delivering the highest energy saving potential varies for the different slat tilt angles, however, no matter what transition temperature is applied to the TT material, none of the TT PS-TIM windows with tilted slats could improve upon the energy saving potential of the window with non-tilted slats.

The effect on daylight availability of altering the transition temperature of the TT layer on the tilted slats is given in Fig. 17. It may be seen that in general, as the transition temperature increases, and the TT layer spends increasingly longer in its clear state, the UDI<sub>500-2000lux</sub> drops in the region next to the window (as it becomes subject to increased hours of over illumination) and increases towards the rear of the office (which benefits from the increased levels of light entering via the window).

**Table 2**

Energy saving potential and average UDI for an office space served by 5 mm TT PS-TIM windows with various optical properties and switching temperatures.

Energy saving potential				Transition temperature	Average UDI			
t 10%	t 20%	t 30%	t 40%		t 10%	t 20%	t 30%	t 40%
-8.0%	-5.5%	-0.5%	6.8%	19°C	48.5%	53.1%	55.9%	58.1%
-3.7%	-1.1%	3.9%	11.0%	21°C	50.9%	55.2%	57.7%	59.1%
0.7%	3.2%	8.0%	14.6%	23°C	52.1%	55.6%	57.4%	58.3%
3.2%	5.7%	10.4%	16.5%	25°C	52.6%	55.5%	56.8%	57.2%
4.5%	7.1%	11.6%	17.0%	27°C	52.7%	54.8%	55.8%	55.7%
5.8%	7.9%	12.2%	17.0%	29°C	52.8%	54.2%	54.6%	54.1%
6.3%	8.1%	11.9%	16.4%	31°C	51.5%	52.5%	52.5%	51.8%

**Table 3**

Energy saving potential and average UDI for an office space served by 7.5 mm TT PS-TIM windows with various optical properties and switching temperatures.

Energy saving potential				Transition temperature	Average UDI			
t 10%	t 20%	t 30%	t 40%		t 10%	t 20%	t 30%	t 40%
8.8%	12.9%	17.4%	19.2%	19°C	49.6%	59.1%	56.8%	55.4%
12.1%	15.9%	19.4%	21.3%	21°C	50.9%	58.6%	55.9%	54.3%
13.9%	17.2%	20.1%	22.0%	23°C	51.9%	57.1%	54.0%	52.5%
14.3%	17.1%	19.5%	20.9%	25°C	51.5%	54.9%	51.7%	50.0%
14.0%	15.7%	17.3%	19.9%	27°C	51.1%	52.1%	49.9%	47.6%
12.8%	13.1%	15.9%	17.7%	29°C	49.5%	49.8%	47.6%	45.5%
11.6%	11.4%	13.4%	15.6%	31°C	47.3%	46.3%	44.2%	43.1%

**Table 4**

Energy saving potential and average UDI for an office space served by 10 mm TT PS-TIM windows with various optical properties and switching temperatures.

Energy saving potential				Transition temperature	Average UDI			
t 10%	t 20%	t 30%	t 40%		t 10%	t 20%	t 30%	t 40%
16.2%	17.8%	19.3%	20.9%	19°C	57.7%	55.4%	52.5%	49.0%
17.7%	19.0%	20.3%	21.7%	21°C	56.5%	54.0%	51.2%	48.4%
17.9%	19.0%	20.2%	21.3%	23°C	54.3%	51.7%	49.0%	45.6%
16.9%	17.9%	18.9%	19.9%	25°C	52.1%	49.6%	46.8%	43.6%
15.7%	16.2%	17.7%	18.8%	27°C	50.0%	47.2%	43.2%	41.2%
13.9%	13.5%	15.8%	16.5%	29°C	47.5%	44.9%	41.3%	39.7%
11.7%	11.9%	13.5%	15.4%	31°C	44.8%	42.3%	39.4%	37.8%

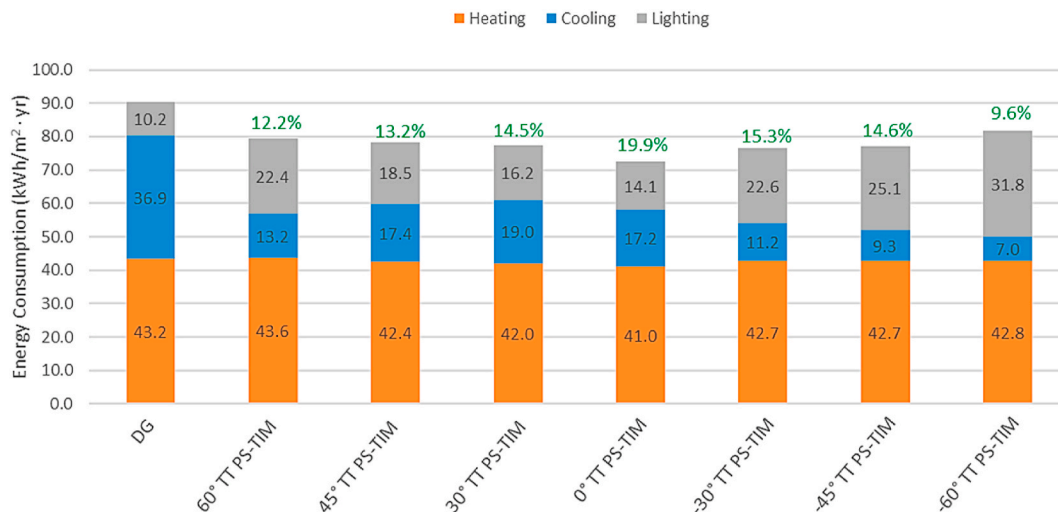


**Fig. 14.** Annual heating, cooling and lighting energy consumption of an office space served by TT PS-TIM windows with different slat tilt angles for a slat spacing of 10 mm.

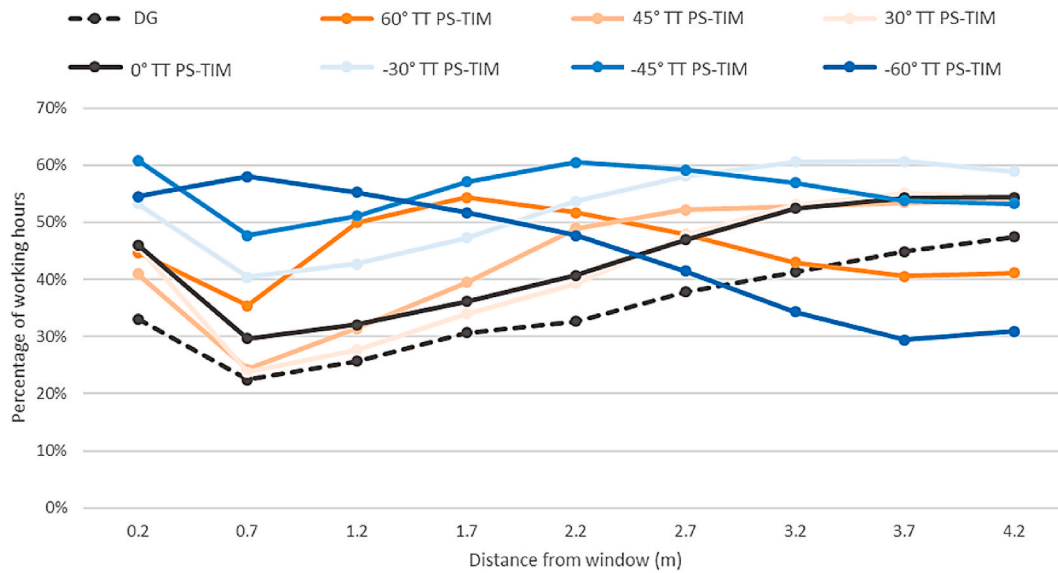


Fig. 15. UDI<sub>500–2000 lux</sub> distribution in an office space served by TT PS-TIM windows with different slat tilt angles for a slat spacing of 10 mm.

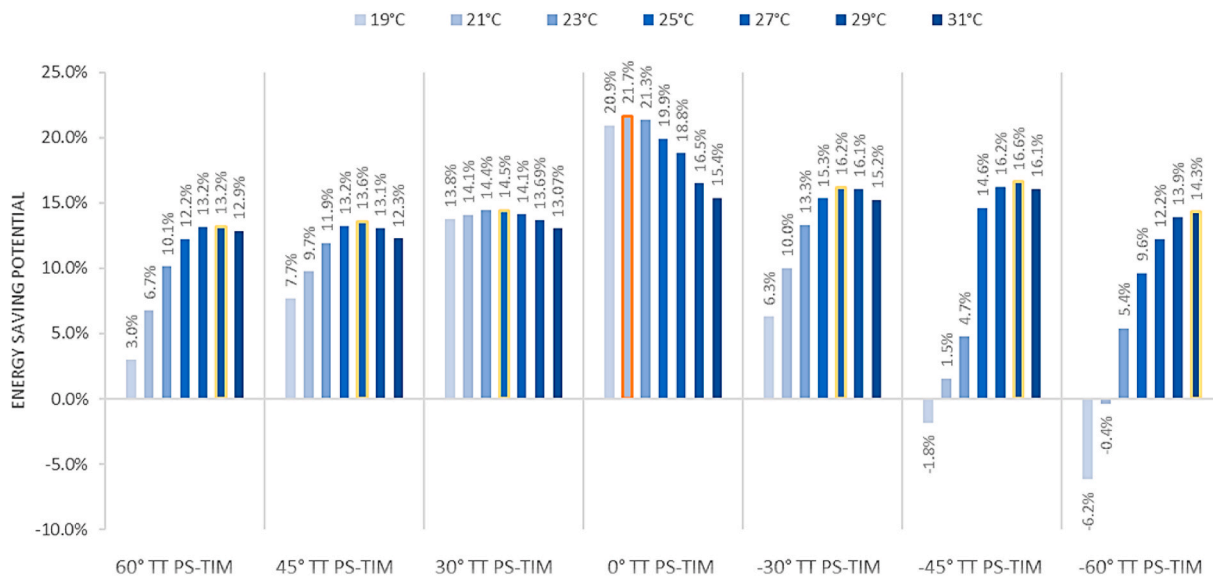


Fig. 16. Annual energy saving potential for an office served by TT PS-TIM windows with different slat tilt angles and varying TT transition temperatures for a slat spacing of 10 mm.

The general pattern of behaviour and its causes echo the observations made in section 4.2.1 and it may be seen that the best performing window from that section (i.e.  $-30^\circ$ ), offers continuing improvements in lighting levels as the transition temperature is decreased in steps to  $19^\circ\text{C}$ . This means more time is spent in the translucent state, protecting the region next to the window, but the geometry of the slats means that a significant proportion of the incident light passes through just one slat, attenuation is lower than for the other slat angles, and more light is available to illuminate the rear of the office.

As with previous scenarios, it is important to interpret the UDI results alongside the data for lighting energy demand, which may be optimal for a different window design.

#### 4.2.3. Optimized design scenarios

Tables 5 and 6 summarise the energy saving potential and average UDI for the office served by TT PS-TIM windows with different slat tilt angles. Data for the TT PS-TIM window with non-tilted slats is provided for comparison and it may be seen that while its energy saving potential

is high, it delivers poor daylight performance. Of the TT PS-TIM windows with tilted slats, only those with  $-30^\circ$  and  $-45^\circ$  tilt angles offer improved daylight performance, however, the transition temperatures that lead to good daylight availability, deliver poor energy savings. Thus, it can be concluded that for a 10 mm slat spacing, TT PS-TIM with tilted slats do not provide simultaneous improvements in energy efficiency and luminous quality when compared with TT PS-TIM with non-tilted slats. This means for the 10mm slat spacing an optimized design cannot be achieved with titled slats.

### 5. Conclusions

Applying a novel window system incorporating a thermotropic (TT) material and Transparent Insulation Material (TIM) can simultaneously achieve dynamic daylight and solar heat gain regulation, reduce building energy consumption, and improve the luminous environment in a space modelled on a small cellular office. This research investigated the effects of geometric configuration and thermotropic features on building

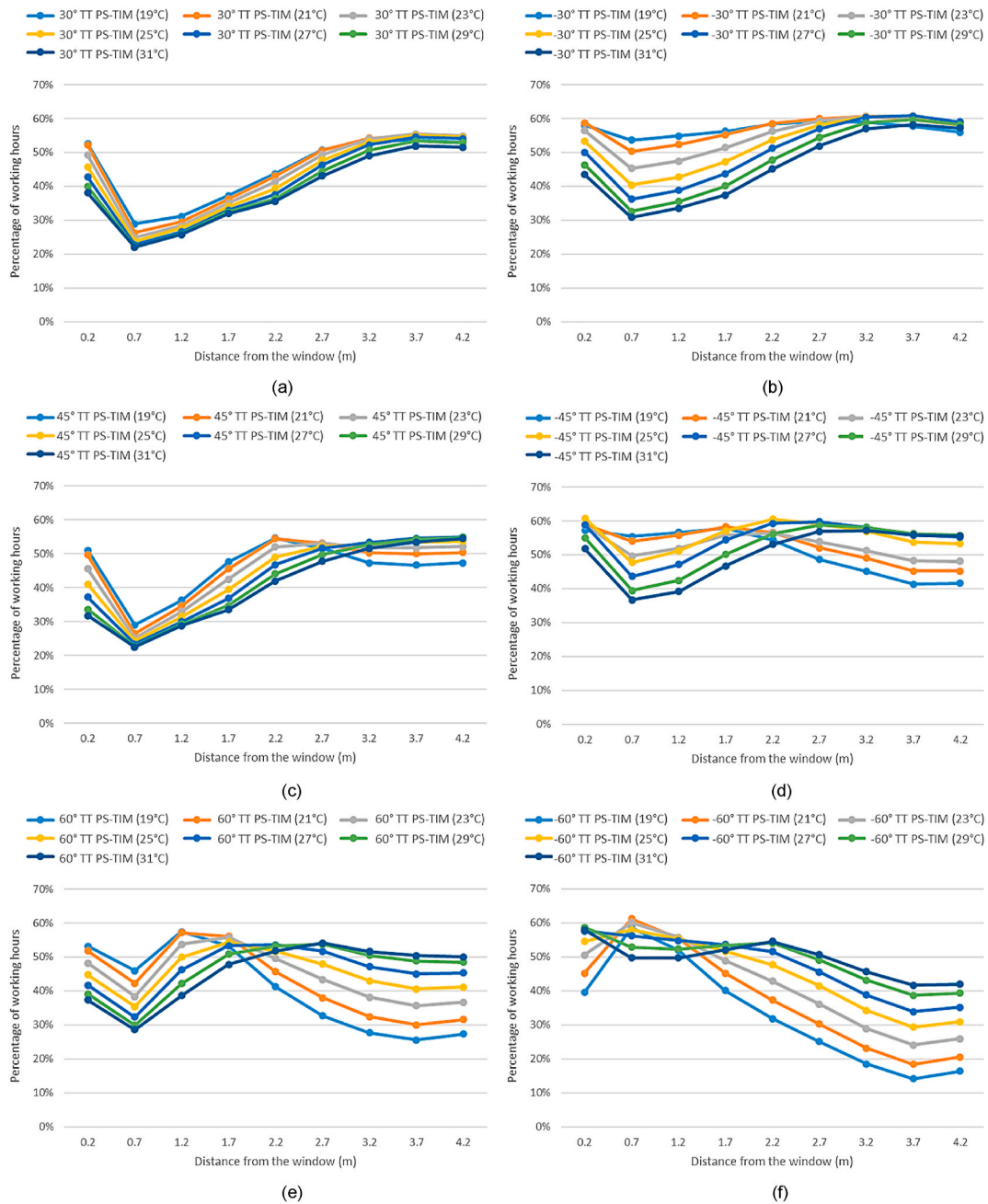


Fig. 17. UDI<sub>500-2000lux</sub> distribution for an office served by TT PS-TIM windows with different slat tilt angles and varying TT transition temperatures for a slat spacing of 10 mm.

performance through a comprehensive workflow.

For the space investigated, the following conclusions can be drawn: 1) both the slat spacing and slat tilt angle show important influence on energy and daylight performance; 2) the TT material transition temperature and optical properties significantly affect TT PS-TIM’s building performance for a given geometric configuration, and varying the thermotropic properties was found to deliver results that showed up to 25% difference in energy saving potential between the best and the worst performing cases; 3) a smaller slat spacing delivers a better quality of luminous environment (as quantified by UDI) but the energy efficiency, based on heating, cooling and lighting demand, is worse than for wider slat spacings: a 7.5 mm TT PS-TIM window with non-tilted slats, given the appropriate thermotropic properties was found to deliver the optimal energy and daylight performance with an energy saving potential of up to 22% when compared with a conventional double-glazed

window, and an average UDI<sub>500-2000lux</sub> of 59%; 4) for a 10 mm slat spacing, neither TT PS-TIM windows with positive slat tilt angles (tilted towards the sky vault), or negative slat tilt angles (tilted away from the sky vault), were found to offer better performance in terms of both energy efficiency and daylight quality than TT PS-TIM with non-tilted slats.

This analysis of the combined influence of the TT PS-TIM window geometric configuration and thermotropic features aims to offer some tentative suggestions as to how a novel window system with TT PS-TIM might be designed. To reach the stage of marketable products, investigations into manufacturing feasibility and long-term durability of the systems need to be undertaken.

The research presented in this paper limited itself to an unshaded south-facing room based on a cellular office located in London. The performance of building integrated TT PS-TIM window system at other

**Table 5**

Energy saving potential for an office served by TT PS-TIM windows with different slat tilt angles and TT transition temperatures, and a slat spacing of 10 mm.

	Energy Saving potential						
	60°	45°	30°	0°	-30°	-45°	-60°
19°C	3.0%	7.7%	13.8%	20.9%	6.27%	-1.8%	-6.2%
21°C	6.7%	9.7%	14.1%	21.7%	9.99%	1.5%	-0.4%
23°C	10.1%	11.9%	14.4%	21.3%	13.28%	4.7%	5.4%
25°C	12.2%	13.2%	14.5%	19.9%	15.34%	14.6%	9.6%
27°C	13.2%	13.6%	14.1%	18.8%	16.20%	<b>16.2%</b>	12.2%
29°C	13.2%	13.1%	13.69%	16.5%	16.07%	16.6%	13.9%
31°C	12.9%	12.3%	13.07%	15.4%	15.20%	16.1%	14.3%

**Table 6**

Average UDI for an office served by TT PS-TIM windows with different slat tilt angles and TT transition temperatures, and a slat spacing of 10 mm.

	Average UDI						
	60°	45°	30°	0°	-30°	-45°	-60°
19°C	40.5%	45.7%	44.9%	49.0%	57.0%	50.9%	32.9%
21°C	42.8%	46.1%	44.6%	48.4%	57.0%	52.8%	37.4%
23°C	44.4%	45.2%	43.6%	45.6%	55.1%	52.7%	41.5%
25°C	45.4%	44.1%	42.3%	43.6%	52.8%	55.6%	44.8%
27°C	46.3%	43.2%	41.1%	41.2%	50.8%	<b>54.7%</b>	47.5%
29°C	46.3%	41.8%	39.8%	39.7%	48.1%	52.5%	49.1%
31°C	45.6%	40.7%	38.8%	37.8%	46.1%	50.3%	49.3%

orientations and under different climates will be investigated in further research. Detailed evaluation of the discomfort glare (from direct sun and from diffuse light from a translucent window) related to TT PS-TIM window systems, and the effects on visual connectivity into or out of a space, which have a significant effect on the outcome of the design recommendations, will also be included in further research.

#### Declaration of competing interest

The authors declare that they have no known competing financial interests or personal relationships that could have appeared to influence the work reported in this paper.

#### Acknowledgements

This work was supported by the Engineering and Physical Sciences Research Council, UK [grant number EP/S030786/1].

#### References

- S. Nishikawa, et al., Experimental and numerical study of heat transfer from a window with an internal Venetian blind, *Energy Build.* (2020) 223.
- M. Amirkhani, et al., Innovative window design strategy to reduce negative lighting interventions in office buildings, *Energy Build.* 179 (2018) 253–263.
- J. Pereira, et al., Thermal, luminous and energy performance of solar control films in single-glazed windows: use of energy performance criteria to support decision making, *Energy Build.* 198 (2019) 431–443.
- W.H. Ko, et al., The Impact of a View from a Window on Thermal Comfort, Emotion, and Cognitive Performance, *Building and Environment*, 2020, p. 175.
- P. Pilechiha, et al., Multi-objective optimisation framework for designing office windows: quality of view, daylight and energy efficiency, *Appl. Energy* (2020) 261.
- I. Konstantzos, et al., View clarity index: a new metric to evaluate clarity of view through window shades, *Build. Environ.* 90 (2015) 206–214.
- K. Allen, et al., Smart windows—dynamic control of building energy performance, *Energy Build.* 139 (2017) 535–546.
- T. Inoue, M. Ichinose, N. Ichikawa, Thermotropic glass with active dimming control for solar shading and daylighting, *Energy Build.* 40 (3) (2008) 385–393.
- R. Liang, et al., An exploration of the combined effects of NIR and VIS spectrally selective thermochromic materials on building performance, *Energy Build.* 201 (2019) 149–162.
- R.S. Zakirullin, Chromogenic materials in smart windows for angular-selective filtering of solar radiation, *Materials Today Energy* 17 (2020).
- G. Ciampi, et al., Thermal Model Validation of an Electric-Driven Smart Window through Experimental Data and Evaluation of the Impact on a Case Study, *Building and Environment*, 2020, p. 181.
- K. Resch, G.M. Wallner, Thermotropic layers for flat-plate collectors—a review of various concepts for overheating protection with polymeric materials, *Sol. Energy Mater. Sol. Cell.* 93 (1) (2009) 119–128.
- K. Connelly, et al., Design and development of a reflective membrane for a novel building integrated concentrating photovoltaic (BICPV) ‘smart window’ system, *Appl. Energy* 182 (2016) 331–339.
- Y. Wu, et al., Smart solar concentrators for building integrated photovoltaic façades, *Sol. Energy* 133 (2016) 111–118.
- K. Resch-Fauster, et al., Thermotropic overheating protection for façade-integrated solar thermal collectors, *Sol. Energy Mater. Sol. Cell.* 170 (2017) 39–47.
- J. Yao, N. Zhu, Evaluation of indoor thermal environmental, energy and daylighting performance of thermotropic windows, *Build. Environ.* 49 (2012) 283–290.
- P. Nitz, H. Hartwig, Solar control with thermotropic layers, *Sol. Energy* 79 (6) (2005) 573–582.
- J.F. Peter Nitz, Stangl Rolf, Helen Rose Wilson, Volker Wittwer, Simulation of multiply scattering media, *Sol. Energy Mater. Sol. Cell.* 54 (1–4) (1998) 297–307.
- H. Wilson, J. Ferber, W. Platzer, Optical properties of thermotropic layers, in: *Optical Materials Technology for Energy Efficiency and Solar Energy Conversion XIII*, 2255, SPIE, 1994.
- H. Wilson, Potential of thermotropic layers to prevent overheating: a review, in: *Optical Materials Technology for Energy Efficiency and Solar Energy Conversion XIII*, 2255, SPIE, 1994.
- W.G. Andreas Georg, Dietmar Schweiger, Volker Wittwer, Peter Nitz, Helen Rose Wilson, Switchable glazing with a large dynamic range in total solar energy transmittance (TSET), *Sol. Energy* 62 (3) (1998) 215–228.
- H.R.W. Alexandra Raicu, Peter Nitz, Platzer Werner, Volker Wittwer, Ekkehard Jahns, Facade systems with variable solar control using thermotropic polymer blends, *Sol. Energy* 72 (1) (2002) 31–42.
- Y. Nishio, R. Chiba, Y. Miyashita, K. Oshima, T. Miyajima, N. Kimura, H. Suzuki, Salt addition effects on mesophase structure and optical properties of aqueous hydroxypropyl cellulose solutions, *Polym. J.* 34 (3) (2002), 149–157.

- [24] M. Wang, et al., Binary solvent colloids of thermosensitive poly(N-isopropylacrylamide) microgel for smart windows, *Ind. Eng. Chem. Res.* 53 (48) (2014) 18462–18472.
- [25] X.-H. Li, et al., Broadband light management with thermochromic hydrogel microparticles for smart windows, *Joule* 3 (1) (2019) 290–302.
- [26] V.A. Maiorov, Optical properties of thermotropic hydrogels (a review), *Opt Spectrosc.* 128 (3) (2020) 367–386.
- [27] K. Resch, G.M. Wallner, R.W. Lang, Spectroscopic investigations of phase-separated thermotropic layers based on UV cured acrylate resins, *Macromol. Symp.* 265 (1) (2008) 49–60.
- [28] K.G.T. Hollands, Honeycomb devices in flat plate solar collectors, *Sol. Energy* 21 (1965).
- [29] H. Tabor, Cellular insulation (honeycombs), *Sol. Energy* 12 (4) (1969) 549–552.
- [30] G. Francia, A new collector of solar radiant energy: theory and experimental verification, in: *Proceedings of the United Nations Conference on New Sources of Energy*, vol. 4, 1961 (Rome).
- [31] N.D. Kaushika, P. Kumar, Convective effects in air layers bound by cellular honeycomb arrays, *J. Sci. Ind. Res.* 64 (2005) 602–612.
- [32] A.A. Ghoneim, Performance optimization of solar collector equipped with different arrangements of square-celled honeycomb, *Int. J. Therm. Sci.* 44 (1) (2005) 95–105.
- [33] H. Suehrcke, et al., Heat transfer across corrugated sheets and honeycomb transparent insulation, *Sol. Energy* 76 (1–3) (2004) 351–358.
- [34] M. Arulanantham, N.D. Kaushika, Coupled radiative and conductive thermal transfers across transparent honeycomb insulation materials, *Appl. Therm. Eng.* 16 (3) (1996) 209–212.
- [35] N.D. Kaushika, et al., Transparent insulation characteristics of honeycomb and slat arrays, *Energy Build.* 19 (10) (1994) 1037–1041.
- [36] A. Goetzberger, *Transparent Insulation Technology for Solar Energy Conversion*, second ed., Fraunhofer Institute for Solar Energy Systems, Freiburg, 1991.
- [37] W.J. Platzer, Directional-hemispherical solar transmittance data for plastic type honeycomb structures, *Sol. Energy* 49 (1992).
- [38] W.J. Platzer, Calculation procedure for collectors with a honeycomb cover of rectangular cross section, *Sol. Energy* 48 (1992).
- [39] N.D. Kaushika, R. Padmapriya, Solar Transmittance of Honeycomb and Parallel Slat Arrays, *Energy Conversion and Management*, 1991, p. 32.
- [40] W.J. Platzer, Solar transmittance of transparent insulation materials, *Sol. Energy Mater.* 16 (1987).
- [41] K.G.T. Hollands, K.N. Marshall, R.K. Wedel, An approximate equation for predicting the solar transmittance of transparent honeycombs, *Sol. Energy* 21 (3) (1978) 231–236.
- [42] K.G.T. Hollands, K. I. C. Ford, W.J. Platzer, Manufacture, solar transmission, and heat transfer characteristics of large-celled honeycomb transparent insulation, *Sol. Energy* 49 (5) (1992) 381–385.
- [43] G.M. Wallner, W. Platzer, R.W. Lang, Structure–property correlations of polymeric films for transparent insulation wall applications. Part 1: solar optical properties, *Sol. Energy* 79 (6) (2005) 583–592.
- [44] G.M. Wallner, W. Platzer, R.W. Lang, Structure–property correlations of polymeric films for transparent insulation wall applications. Part 2: infrared optical properties, *Sol. Energy* 79 (6) (2005) 593–602.
- [45] G.M. Wallner, et al., Development and application demonstration of a novel polymer film based transparent insulation wall heating system, *Sol. Energy Mater. Sol. Cell.* 84 (1–4) (2004) 441–457.
- [46] Y. Sun, et al., Development of a comprehensive method to analyse glazing systems with Parallel Slat Transparent Insulation material (PS-TIM), *Appl. Energy* 205 (2017) 951–963.
- [47] Y. Sun, Y. Wu, R. Wilson, Analysis of the daylight performance of a glazing system with parallel slat transparent insulation material (PS-TIM), *Energy Build.* 139 (2017) 616–633.
- [48] Y. Sun, et al., Glazing systems with parallel slats transparent insulation material (PS-TIM): evaluation of building energy and daylight performance, *Energy Build.* 159 (2018) 213–227.
- [49] Y. Sun, R. Wilson, Y. Wu, A Review of Transparent Insulation Material (TIM) for building energy saving and daylight comfort, *Appl. Energy* 226 (2018) 713–729.
- [50] I.L. Wong, P.C. Eames, R.S. Perera, A review of transparent insulation systems and the evaluation of payback period for building applications, *Sol. Energy* 81 (9) (2007) 1058–1071.
- [51] A. Paneri, I.L. Wong, S. Burek, Transparent insulation materials: an overview on past, present and future developments, *Sol. Energy* 184 (2019) 59–83.
- [52] D. Liu, et al., Comprehensive evaluation of window-integrated semi-transparent PV for building daylight performance, *Renew. Energy* 145 (2020) 1399–1411.
- [53] K. Connelly, et al., Transmittance and reflectance studies of thermotropic material for a novel building integrated concentrating photovoltaic (BICPV) ‘smart window’ system, *Energies* 10 (11) (2017).
- [54] S. Crone, *Radiance Users Manual*, 1992.
- [55] A. McNeil, et al., A validation of a ray-tracing tool used to generate bi-directional scattering distribution functions for complex fenestration systems, *Sol. Energy* 98 (2013) 404–414.
- [56] A. McNeil, E.S. Lee, A validation of the Radiance three-phase simulation method for modelling annual daylight performance of optically complex fenestration systems, *Journal of Building Performance Simulation* 6 (1) (2013) 24–37.
- [57] M. Andersen, et al., Bi-directional transmission properties of Venetian blinds: experimental assessment compared to ray-tracing calculations, *Sol. Energy* 78 (2) (2005) 187–198.
- [58] M. Andersen, M. Rubin, J.-L. Scartezzini, Comparison between ray-tracing simulations and bi-directional transmission measurements on prismatic glazing, *Sol. Energy* 74 (2) (2003) 157–173.
- [59] M. Andersen, J. de Boer, Goniophotometry and assessment of bidirectional photometric properties of complex fenestration systems, *Energy Build.* 38 (7) (2006) 836–848.
- [60] Y. Sun, et al., Experimental measurement and numerical simulation of the thermal performance of a double glazing system with an interstitial Venetian blind, *Build. Environ.* 103 (2016) 111–122.
- [61] Y. Sun, et al., Thermal evaluation of a double glazing façade system with integrated Parallel Slat Transparent Insulation Material (PS-TIM), *Build. Environ.* 105 (2016) 69–81.
- [62] ASHRAE, Standard Method of Test for the Evaluation of Building Energy Analysis Computer Programs, American Society of Heating, Refrigerating and Air-Conditioning Engineers, Inc, 2004.
- [63] H. Tian, et al., Study on the energy saving potential for semi-transparent PV window in southwest China, *Energies* 11 (11) (2018) 3239.
- [64] IEA and ECBCS, in: P. Bhusal (Ed.), Annex 45 Energy Efficient Electric Lighting for Buildings: Lighting Energy in Buildings in Guidebook On Energy Efficient Electric Lighting For Buildings, Liisa Halonen, Eino Tetri, 2006. France.
- [65] M. Sheppy, L. Gentile-Polese, S. Gould, Plug and Process Loads Capacity and Power Requirements Analysis, U.S. Department of Energy, 2014.
- [66] A. McNeil, The Three-phase Method for Simulation Complex Fenestration with Radiance, 2014.
- [67] M. Saxena, et al., Dynamic RADIANCE – predicting annual daylight with variable fenestration optics using BSDFs, in: Fourth National Conference of IBPSA-USA, 2010 (New York City, USA).
- [68] M. Konstantoglou, J. Jonsson, E. Lee, Simulating complex window systems using BSDF data, in: 26th Conference on Passive and Low Energy Architecture, 2009. Quebec City, Canada.
- [69] J.M. Azza Nabil, Useful daylight illuminances: a replacement for daylight factors, *Energy Build.* 38 (2006) 905–913.